Electronic Supplementary Information

Synthesis of zirconocene complexes and their use in slurry-phase polymerisation of ethylene

Phakpoom Angpanitcharoen, Jessica V. Lamb, Zoë R. Turner, Jean-Charles Buffet, and Dermot O'Hare*

Chemistry Research Laboratory, Department of Chemistry, University of Oxford, 12 Mansfield Road, Oxford, OX1 3TA, United Kingdom. Tel: +44(0) 1865 272686; E-mail: dermot.ohare@chem.ox.ac.uk

Table of Contents

1. Experimental details

1.1 Air- and moisture-sensitive compounds

Air- and moisture-sensitive compounds were handled under an inert N_2 atmosphere, using standard Schlenk line techniques and an MBraun Unilab glove box where required. All glassware was dried in an oven at 160 °C for a minimum of two hours prior to use. Molecular sieves (3 Å, 8-12 mesh) were supplied by ACROS Organics and dried at 140 °C *in vacuo* for 16 hours prior to use.

1.2 Commercially supplied reagents

Oxalyl chloride (Alfa Aesar), (E)-α-methylcinnamic acid (Sigma Aldrich), N,N-dimethylformamide (Sigma Aldrich), anhydrous $AlCl_3$ (Sigma Aldrich), $LiAlH_4$ (2.0 M in THF, Sigma Aldrich), ^{n}BuLi (2.5 M in hexanes, Sigma Aldrich), triisobutylaluminium (Sigma Aldrich), 1,2,3,4-tetramethylbenzene (SCG Chemicals Co., Ltd.), concentrated HCl (Fisher Scientific), anhydrous $MgSO_4$ (Fisher Scientific) concentrated H_2SO_4 (Fisher Scientific), and $NaHCO_3$ (ACROS Organics) were used as supplied. Prior to use, dichlorodiethylsilane (Sigma Aldrich) was dried over molecular sieves and freeze-pump-thaw degassed three times, $ZrBr_4$ (Sigma Aldrich) and $ZrCl_4$ (Sigma Aldrich) were dried at 140 °C for 16 hours, methylaluminoxane (10% wt in toluene, Sigma Aldrich) and polymethylaluminoxane (12.40% wt in toluene, SCG Chemicals Co., Ltd.) were dried *in vacuo*, and ethylene gas (99.9%, BOC Industrial Gases) was passed through a drying column containing molecular sieves.

1.3 Synthesis of literature compounds

KCH_2Ph,[1] and $^{3\text{-Me}}Ind^{\#}Li$[2] were prepared according to literature procedures.

1.4 Solvent preparation

Pentane, hexane, toluene, dichloromethane and benzene were dried using an MBraun SPS-800 solvent purification system and degassed under partial vacuum before use. The non-chlorinated solvents were stored in ampoules over a potassium mirror, while DCM was stored over molecular sieves. Tetrahydrofuran (THF) was distilled from sodium benzophenone ketyl, stored in an ampoule over molecular sieves and degassed under partial vacuum before use. Diethyl ether (Et_2O) was distilled from Na/K, stored in an ampoule over a potassium mirror and degassed under partial vacuum before use.

Benzene-d_6 (99.6%, Sigma Aldrich) was dried over Na/K and chloroform-d_1 (99.8%, Sigma Aldrich) was dried over CaH_2. The deuterated solvents were distilled under static vacuum, freeze-pump-thaw degassed three times and stored over pre-activated 4 Å molecular sieves under N_2.

1.5 Solution phase NMR spectroscopy

NMR spectroscopy samples of air- and moisture-sensitive compounds were prepared using dry deuterated solvents in a glove box and sealed in 5 mm Young's tap NMR tubes. ^{1}H and ^{13}C{^{1}H} NMR spectra were recorded on either a Bruker Avance III HD nanobay 400 MHz or Bruker Avance III 500 MHz NMR spectrometer. All spectra were recorded at 298 K and referenced internally to the residual *protio* solvent resonance. All spectra are reported relative to tetramethylsilane (δ = 0 ppm). Two dimensional ^{1}H-^{1}H and ^{13}C-^{1}H correlation experiments were used, when necessary, to confirm ^{1}H and ^{13}C assignments.

1.6 Elemental analysis

Air and moisture sensitive samples were prepared in a glove box under a N_2 atmosphere and sealed in glass vials. CHN analyses were carried out in duplicate by Mr Stephen Boyer (London Metropolitan University).

1.7 Mass spectrometry (MS)

Samples were prepared in a glove box under a N_2 atmosphere and sealed in glass tubes. Samples were run as electron impact (EI) mass spectra on an Agilent GC-TOF-MS by Dr. James Wickens (University of Oxford) or Mr. Colin Sparrow (University of Oxford).

1.8 Gel-permeation chromatography (GPC)

Gel permeation chromatography (GPC) samples were collected by Ms Liv Thorbu at Norner AS (Norway) on a high temperature gel permeation chromatograph with a IR5 infrared detector (GPC-IR5). Samples were prepared by dissolution in 1,2,4-trichlorobenzene (TCB) containing 300 ppm of 3,5-di-*tert*-butyl-4-hydroxytoluene (BHT) at 160 °C for 90 minutes and then filtered with a 10 µm SS filter before being passed through the GPC column. The samples were run under a flow rate of 0.5 mL/min using TCB containing 300 ppm of BHT as mobile phase with 1 mg/mL BHT added as a flow rate marker. The GPC column and detector temperature were set at 145 and 160 °C respectively.

1.9 Synthesis of PhCH=CMeCOCl

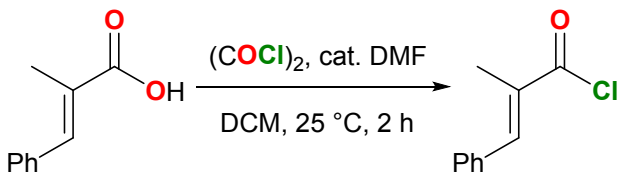

1.0 equivalent (E)-α-methylcinnamic acid (33.6 g, 207 mmol) was dissolved in DCM (500 mL). Under a flow of N_2, 1.1 equivalents oxalyl chloride (28.9 g, 228 mmol) was added to the solution, followed by dry DMF (5 drops), resulting in effervescence. The reaction was stirred for 2 hours at room temperature, with an aliquot confirming that the reaction had gone to completion. ^{1}H NMR (chloroform-d_1, 400 MHz, 298 K) δ (ppm): 8.05 (C=C**H**-Ph, 1H, s), 7.46 (*o,m*-Ph-**H**, 4H, d , $^3J_{HH}$ = 4 Hz), 7.43 (*p*-Ph-**H**, ^{1}H, m), 2.20 (C=C-C**H$_3$**, 3H, s). ^{13}C{^{1}H} NMR (chloroform-d_1, 101 MHz, 298 K) δ (ppm): 170.3 (C=C-**C**OCl), 147.6 (C=**C**H-Ph), 134.6 (C=CH-**Ph**), 132.5 (C=**C**-CH3), 130.2 (*o,m*-**Ph**), 129.9 (*p*-**Ph**), 128.8 (*o,m*-**Ph**), 15.3 (C=C-**C**H$_3$).

1.10 Synthesis of $^{3\text{-Ph}}$Ind$^{\#}$=O

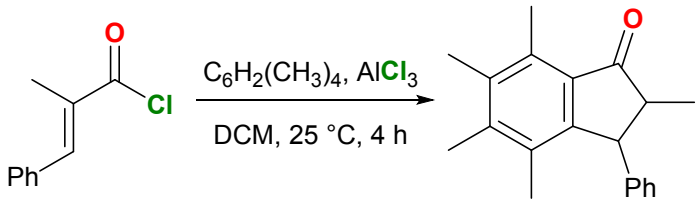

Under a flow of N_2, 1.5 equivalents $AlCl_3$ (41.4 g, 310 mmol) were slowly added a solution of PhCH=CMeCOCl in DCM (500 mL). 0.9 equivalents 1,2,3,4-tetramethylbenzene (25.0 g, 186 mmol) were diluted in DCM (100 mL) and added dropwise to the reaction mixture over 30 minutes, resulting in a colour change from orange to red. The reaction was stirred for 4 hours at room temperature, after which a 1:1 mixture of concentrated HCl and ice (200 mL) was added slowly to quench the reaction, resulting in a colour change from red to light orange. The product was extracted with DCM (3 × 100 mL) and the combined organic layers washed with saturated $NaHCO_3$ solution (100 mL) and deionised water (2 × 100 mL) before being dried using anhydrous $MgSO_4$. The mixture was filtered and the resulting filtrate dried in vacuo to afford $^{3\text{-Ph}}$Ind$^{\#}$=O as a light brown oil in 100% yield (51.9 g, 186 mmol). The crude product contained several diastereomers. Extraction with pentane yielded pure *cis*-$^{3\text{-Ph}}$Ind$^{\#}$=O as a white solid. Colourless crystals of *cis*-$^{3\text{-Ph}}$Ind$^{\#}$=O suitable for a single crystal X-ray diffraction study were grown from hexane at 0 °C. ^{1}H NMR (chloroform-d_1, 400 MHz, 298 K) δ (ppm): 7.18

(*m,p*-Ph-**H**, 3H, m), 6.82 (*o*-Ph-**H**, 2H, bs), 4.61 (C**H**-Ph, 1H, d, $^3J_{HH}$ = 8.2 Hz), 3.00 (C**H**-CH3, 1H, q, $^3J_{HH}$ = 7.3 Hz), 2.71 (Ph-C$\mathbf{H_3}$, 3H, s), 2.27 (Ph-C$\mathbf{H_3}$, 3H, s), 2.24 (Ph-C$\mathbf{H_3}$, 3H,s), 2.00 (Ph-C$\mathbf{H_3}$, 3H, s), 0.81 (CH-C$\mathbf{H_3}$, 3H, d, $^3J_{HH}$ = 7.3 Hz). $^{13}C\{^1H\}$ NMR (chloroform-d_1, 101 MHz, 298 K) δ (ppm): 210.0 (**C**=O), 152.3 (**Ph**), 142.8 (**Ph**), 141.3 (CH-**Ph**), 136.06 (**Ph**), 133.7 (**Ph**), 131.8 (**Ph**), 131.3 (**Ph**), 128.9 (*o*-**Ph**), 128.4 (*m*-**Ph**), 126.5 (*p*-**Ph**), 48.8 (**C**H-CH_3), 48.5 (**C**H-Ph), 17.1 (Ph-**C**H_3), 15.7 (Ph-**C**H_3), 15.6 (Ph-**C**H_3), 14.1 (Ph-**C**H_3), 12.1 (CH-**C**H_3). CHN analysis (%): calculated C 86.29, H 7.97; observed C 84.86, H 7.57. HRMS (ESI): expected *m/z* 301.15629; observed 301.15625 $[M + Na]^+$.

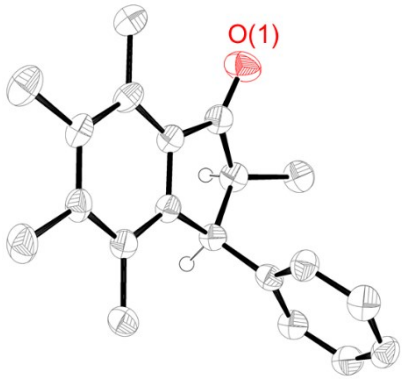

Fig. S1. Molecular structure of *cis*-$^{3\text{-Ph}}$Ind$^{\#}$=O. Hydrogen atoms omitted for clarity (except for stereocentres), ellipsoids drawn at 50% probability. C=O bond length of 1.222(6) Å.

1.11 Synthesis of $^{3\text{-Ph}}$Ind$^{\#}$H

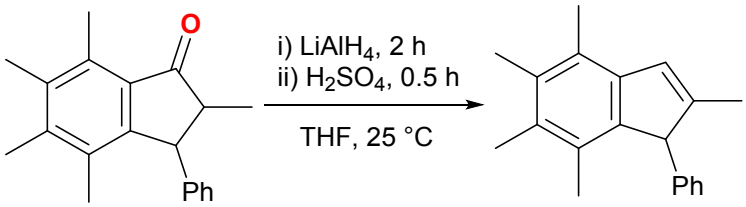

1.0 equivalent $^{3\text{-Ph}}$Ind$^{\#}$=O (54.8 g, 197 mmol) was dissolved in THF (200 mL), forming an orange solution. Under a flow of N_2, 0.5 equivalents $LiAlH_4$ (2.0 M in THF, 49.2 mL, 98.4 mmol) were added dropwise to the solution over 30 minutes and the resulting yellow solution stirred for 2 hours at room temperature. The reaction was cooled to 0 °C and slowly quenched by the addition of 1.0 equivalent deionised water (3.55 mL, 197 mmol). 5.0 equivalents concentrated H_2SO_4 (52.4 mL, 984 mmol) were added dropwise to the reaction mixture over 30 minutes, forming a dark brown solution. The reaction was then quenched with deionised water (200 mL), extracted with DCM (3 × 100 mL) and the combined organic layers washed with saturated $NaHCO_3$ solution (100 mL) and deionised water (2 × 100 mL), dried over anhydrous $MgSO_4$ and filtered. The resulting yellow solution was dried in vacuo to afford

$^{3\text{-Ph}}$Ind$^{\#}$H as a light brown solid in 94% yield (48.8 g, 186 mmol). Colourless crystals of $^{3\text{-Ph}}$Ind$^{\#}$H suitable for a single crystal X-ray diffraction study were grown in hexane at 0 °C. ^{1}H NMR (chloroform-d_1, 400 MHz, 298 K) δ (ppm): 7.20 (*m,p*-Ph-**H**, 3H, m, $^{3}J_{HH}$ = 6.9 Hz), 6.99 (*o*-Ph-**H**, 2H, d, $^{3}J_{HH}$ = 6.9 Hz), 6.56 (C=C-**H**, 1H, s), 4.29 (C**H**-Ph, 1H, s), 2.37 (Ph-C$\mathbf{H_3}$, 3H, s), 2.25 (Ph-C$\mathbf{H_3}$, 3H, s), 2.17 (Ph-C$\mathbf{H_3}$, 3H, s), 1.93 (Ph-C$\mathbf{H_3}$, 3H, s), 1.84 (C=C-C$\mathbf{H_3}$, 3H, s). ^{13}C{^{1}H} NMR (chloroform-d_1, 101 MHz, 298 K) δ (ppm): 148.9 (C=**C**-CH$_3$), 144.0 (**Ph**), 141.8 (**Ph**), 140.5 (CH-**Ph**), 133.8 (**Ph**), 131.3 (**Ph**), 129.6 (**Ph**), 128.6 (*m*-**Ph**), 128.3 (*o*-**Ph**), 126.4 (*p*-**Ph**), 125.3 (C=**C**-H), 125.2 (**Ph**), 60.0 (**C**H-Ph), 16.5 (Ph-**C**H$_3$), 16.4 (Ph-**C**H$_3$), 16.3 (Ph-**C**H$_3$), 16.0 (Ph-**C**H$_3$), 15.4 (C=C-**C**H$_3$). CHN analysis (%): calculated C 91.55, H 8.45; observed C 91.36, H 8.57. HRMS (ESI): expected *m/z* 262.1716; observed 262.1721 [M]$^{+}$.

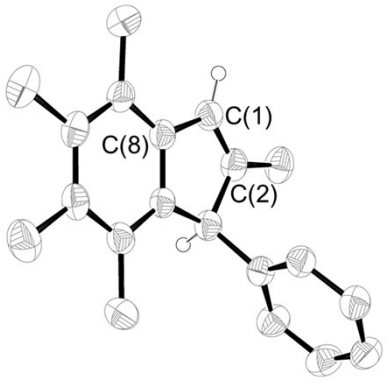

Fig. S2. Molecular structure of $^{3\text{-Ph}}$Ind$^{\#}$H. Hydrogen atoms omitted for clarity (except for stereocentres), ellipsoids drawn at 50% probability. C(1)=C(2) bond length of 1.330(3) Å and C(1)-C(8) bond length of 1.465(2) Å).

1.12 Synthesis of $^{3\text{-Ph}}$Ind$^{\#}$Li

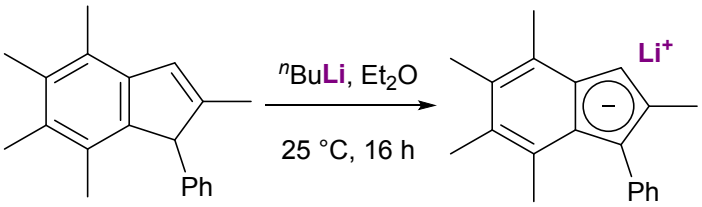

1.0 equivalent $^{3\text{-Ph}}$Ind$^{\#}$H (6.21 g, 23.7 mmol) was dissolved in Et$_2$O (200 mL), forming a yellow solution. 1.5 equivalents ^{n}BuLi (2.5 M in hexanes, 14.2 mL, 35.5 mmol) were added dropwise to the solution at 0 °C. The reaction was allowed to warm up to room temperature and stirred for 16 hours. The resulting yellow suspension was filtered to yield a solid, which was washed with pentane (50 mL) and dried in vacuo to afford $^{3\text{-Ph}}$Ind$^{\#}$Li as an off-white solid in 88% yield (5.62 g, 20.9 mmol). 1H NMR (pyridine-d_5, 400 MHz, 298 K) δ (ppm): 7.78 (*o*-Ph-**H**, 2H, d, $^{3}J_{HH}$ = 7.9 Hz), 7.42 (*m*-Ph-**H**, 2H, dd, $^{3}J_{HH}$ = 7.2, 7.9 Hz), 7.06 (*p*-Ph-**H**, 1H, t, $^{3}J_{HH}$ = 7.2 Hz),

6.67 (Cp-**H**, 1H, s), 2.92 (Cp-C**H$_3$**, 3H, s), 2.86 (Ph-C**H$_3$**, 3H, s), 2.75 (Ph-C**H$_3$**, 3H, s), 2.56 (Ph-C**H$_3$**, 3H, s), 2.55 (Ph-C**H$_3$**, 3H, s). ^{13}C{^{1}H} NMR (pyridine-d_5, 101 MHz, 298 K) δ (ppm): 147.2 (Cp-**Ph**), 132.4 (*o*-**Ph**), 131.9 (**Ph**), 128.5 (**Ph**), 127.3 (**Cp**-CH$_3$), 127.1 (*m*-**Ph**), 122.2 (**Ph**), 120.9 (Ph), 120.5 (*p*-**Ph**), 119.4 (**Ph**), 118.0 (**Ph**), 110.5 (**Cp**-Ph), 96.9 (**Cp**-H), 20.9 (Ph-**C**H$_3$), 18.0 (Cp-**C**H$_3$), 17.7 (Ph-**C**H3), 17.5 (Ph-**C**H$_3$), 17.4 (Ph-**C**H$_3$). ^{7}Li NMR (pyridine-d_5, 156 MHz, 298 K) δ (ppm): 2.58 (s).

2. Abbreviations and numbering

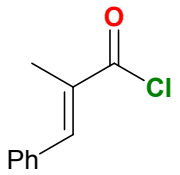

PhCH=CMeOCl

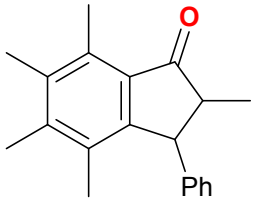

$^{3\text{-Ph}}$Ind$^{\#}$=O

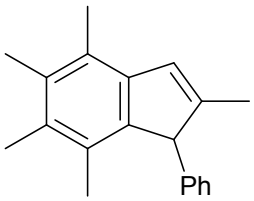

$^{3\text{-Ph}}$Ind$^{\#}$H

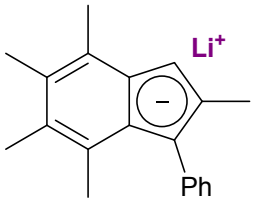

$^{3\text{-Ph}}$Ind$^{\#}$Li

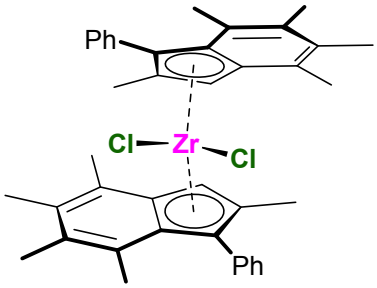

rac-($^{3\text{-Ph}}$Ind$^{\#}$)$_2$ZrCl$_2$
(***rac*-1**)

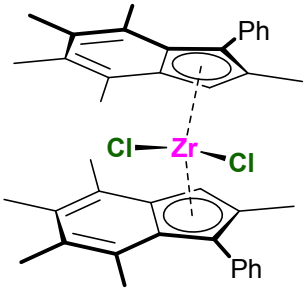

meso-($^{3\text{-Ph}}$Ind$^{\#}$)$_2$ZrCl$_2$
(***meso*-1**)

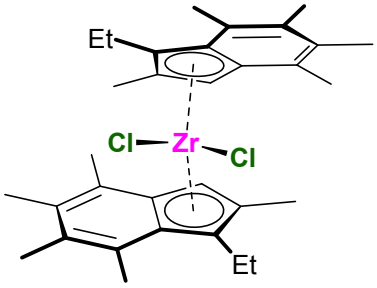

rac-($^{3\text{-Et}}$Ind$^{\#}$)$_2$ZrBr$_2$
(***rac*-2**)

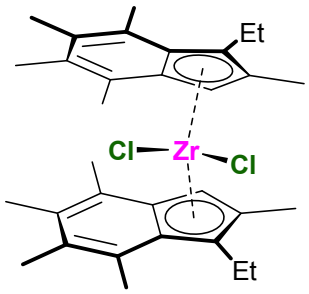

meso-($^{3\text{-Et}}$Ind$^{\#}$)$_2$ZrBr$_2$
(***meso*-2**)

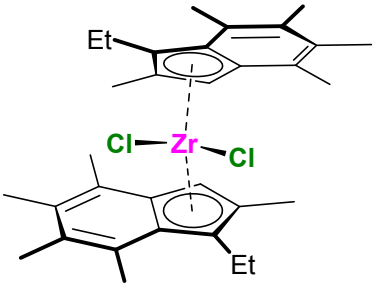

rac-($^{3\text{-Et}}$Ind$^{\#}$)$_2$ZrCl$_2$
(***rac*-3**)

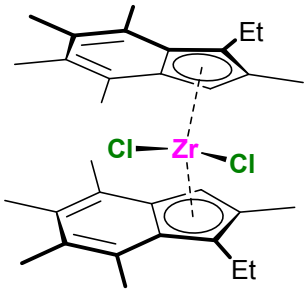

meso-($^{3\text{-Et}}$Ind$^{\#}$)$_2$ZrCl$_2$
(***meso*-3**)

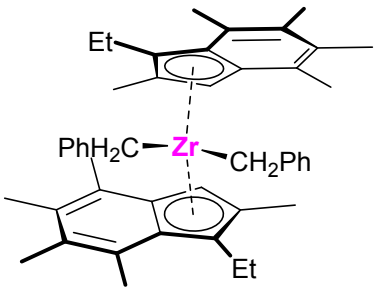

rac-($^{3\text{-Et}}$Ind$^{\#}$)$_2$Zr(CH$_2$Ph)$_2$
(***rac*-4**)

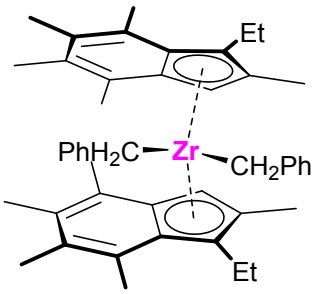

meso-($^{3\text{-Et}}$Ind$^{\#}$)$_2$Zr(CH$_2$Ph)$_2$
(***meso*-4**)

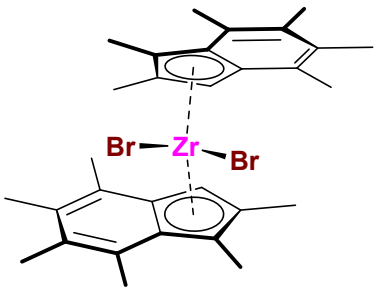

rac-($^{3\text{-Me}}$Ind$^{\#}$)$_2$ZrBr$_2$
(***rac*-5**)

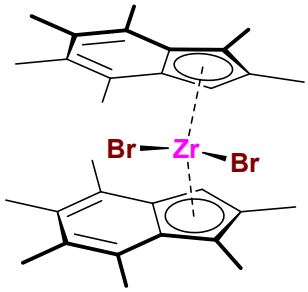

meso-($^{3\text{-Me}}$Ind$^{\#}$)$_2$ZrBr$_2$
(***meso*-5**)

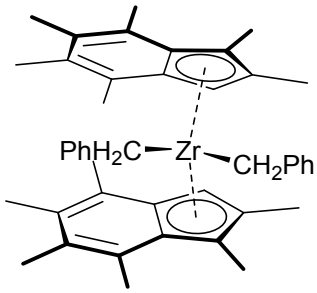

meso-($^{3\text{-Me}}$Ind$^{\#}$)$_2$Zr(CH$_2$Ph)$_2$
(***meso*-6**)

Note: **1** refers to a 50:50 mixture of *rac*-($^{3\text{-Ph}}$Ind$^{\#}$)$_2$ZrCl$_2$ (***rac*-1**) and *meso*-($^{3\text{-Ph}}$Ind$^{\#}$)$_2$ZrCl$_2$ (***meso*-1**).

Chart S1. Ligand and complex structures and numbering system.

3. Representative NMR spectra

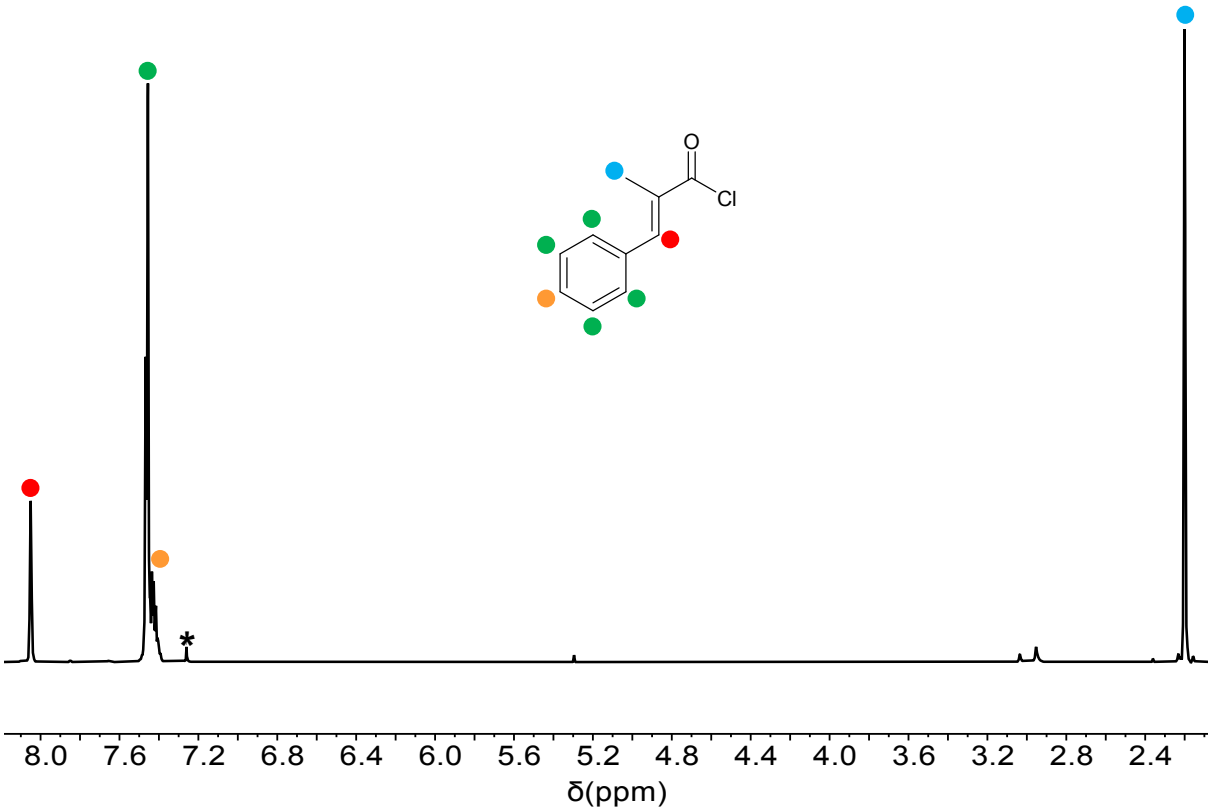

Fig. S3. ^{1}H NMR spectrum (chloroform-d_1 (*), 400 MHz, 298 K) of PhCH=CMeCOCl.

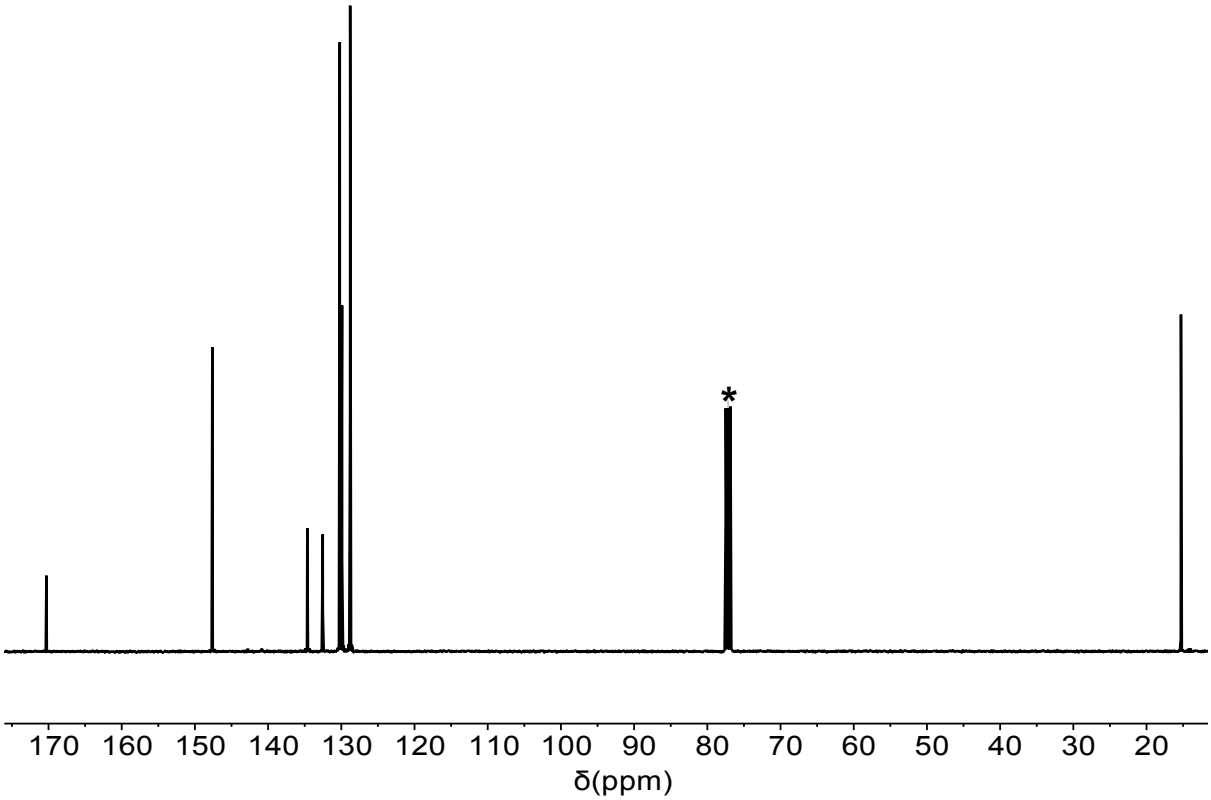

Fig. S4. ^{13}C{^{1}H} NMR spectrum (chloroform-d_1 (*), 101 MHz, 298 K) of PhCH=CMeCOCl.

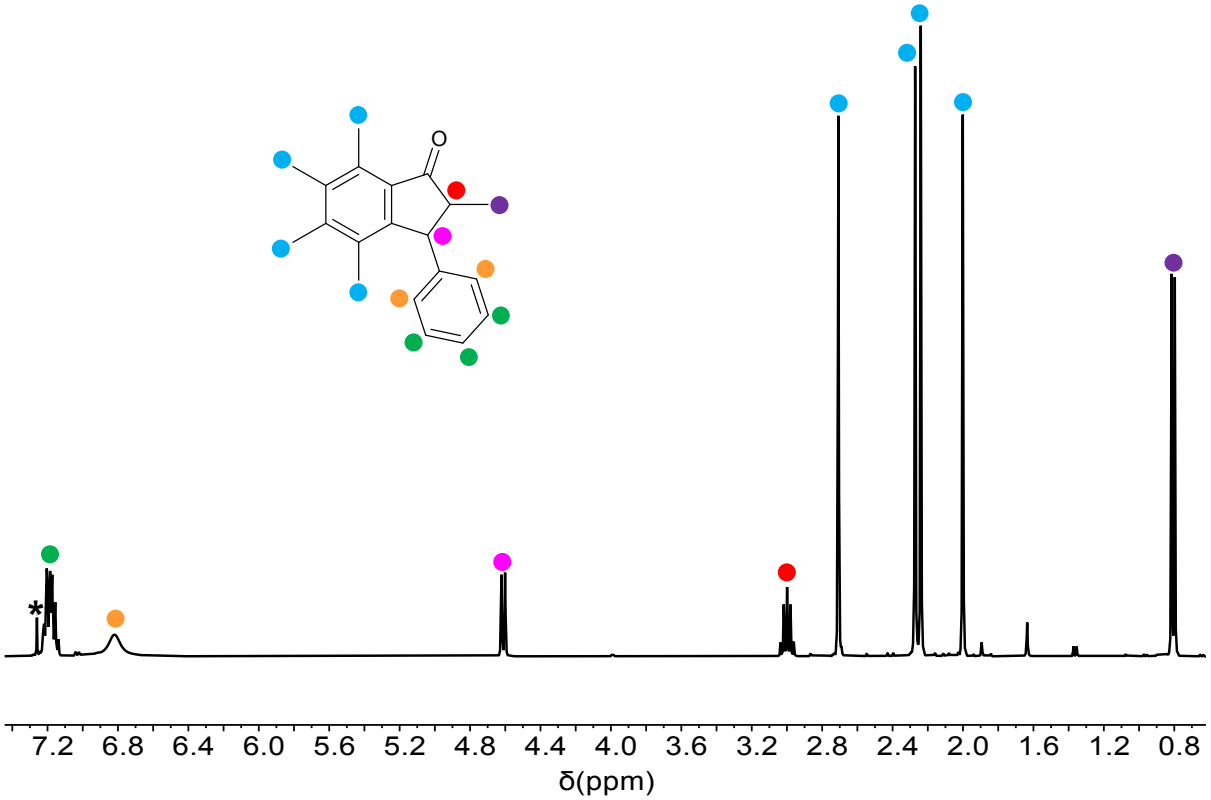

Fig. S5. ^{1}H NMR spectrum (chloroform-d_1 (*), 400 MHz, 298 K) of *cis*-$^{3\text{-Ph}}$Ind$^{\#}$=O.

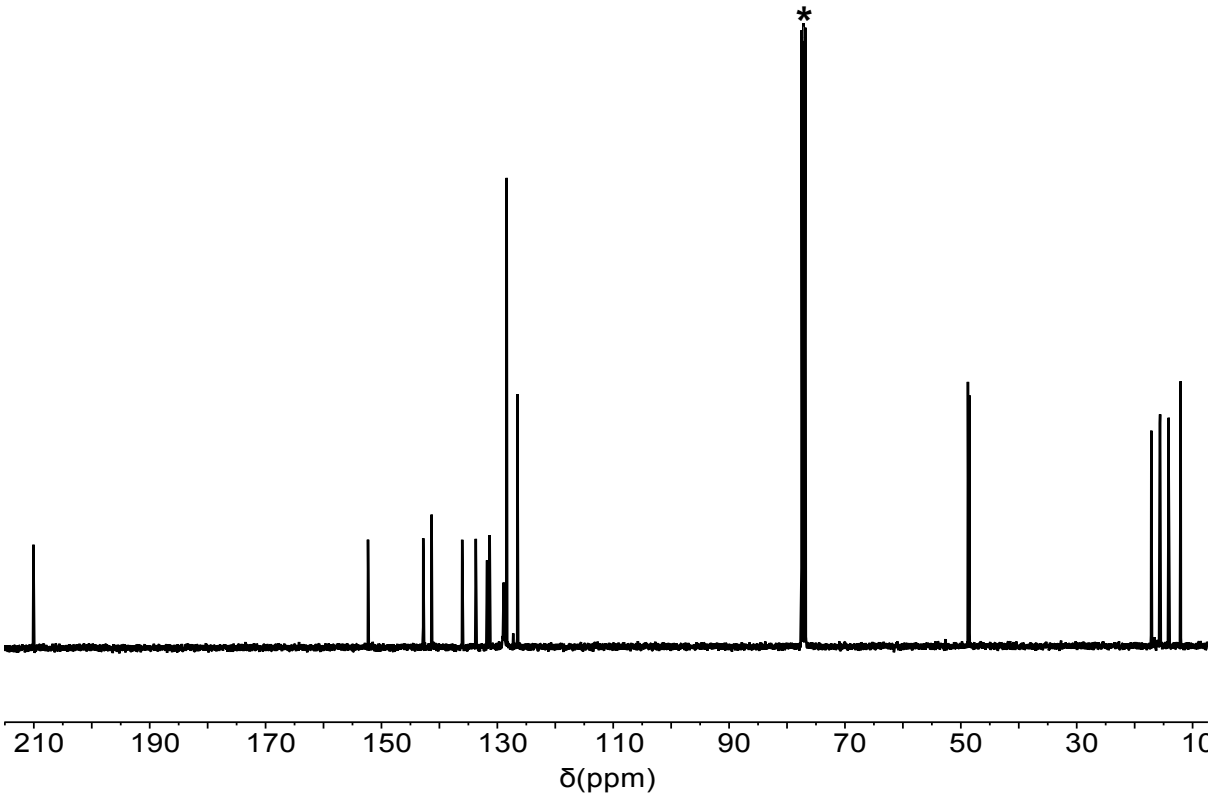

Fig. S6. ^{13}C{^{1}H} NMR spectrum (chloroform-d_1 (*), 101 MHz, 298 K) of *cis*-$^{3\text{-Ph}}$Ind$^{\#}$=O.

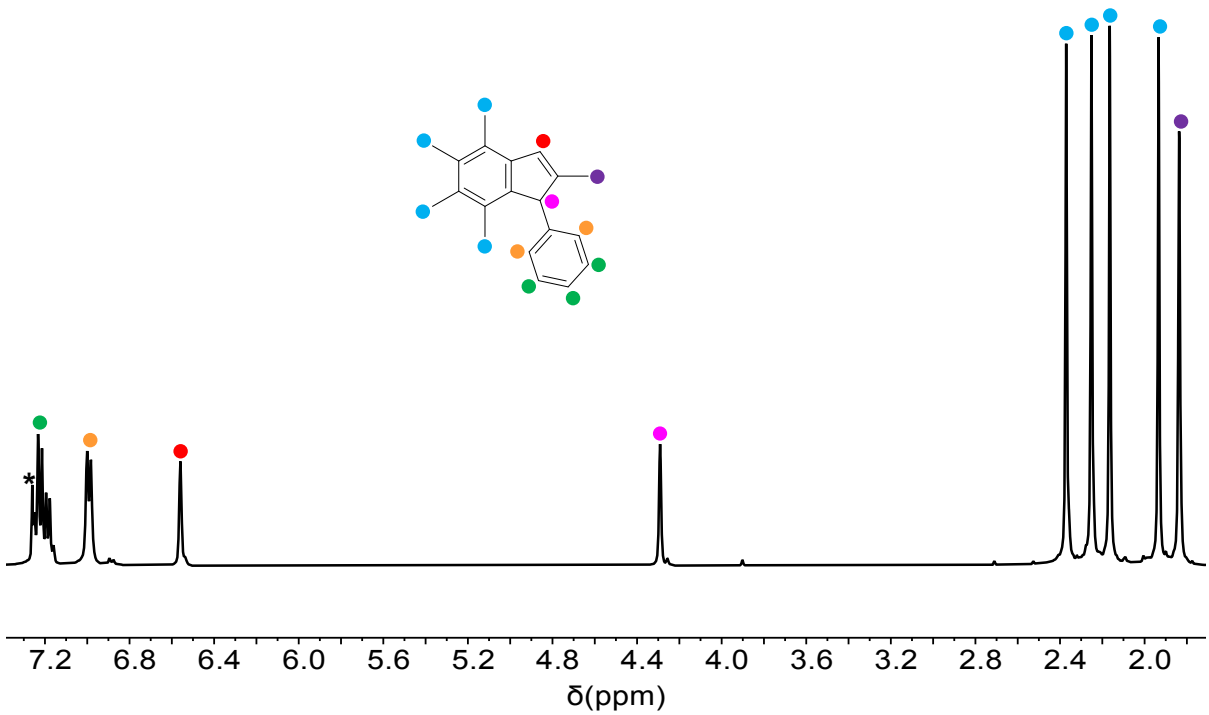

Fig. S7. ^{1}H NMR spectrum (chloroform-d_1 (*), 400 MHz, 298 K) of $^{3\text{-Ph}}$Ind$^{\#}$H.

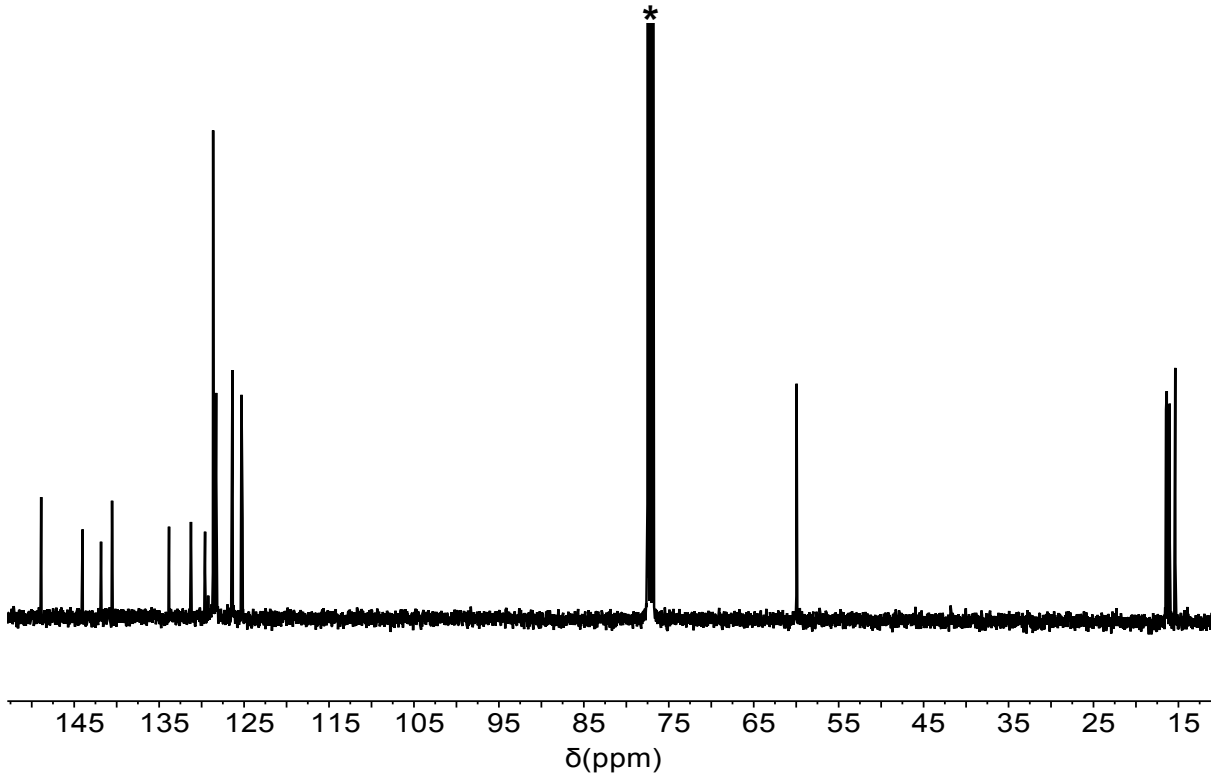

Fig. S8. ^{13}C{^{1}H} NMR spectrum (chloroform-d_1 (*), 101 MHz, 298 K) of $^{3\text{-Ph}}$Ind$^{\#}$H.

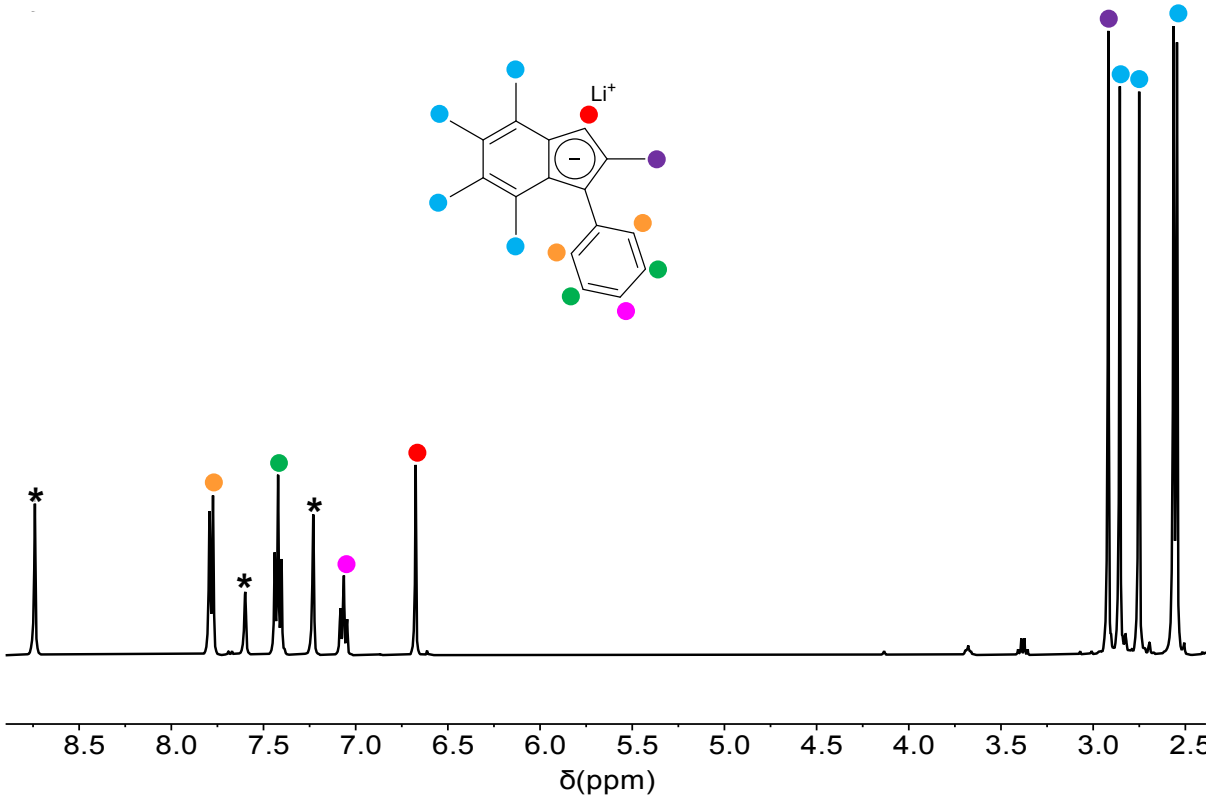

Fig. S9. ^{1}H NMR spectrum (pyridine-d_5 (*), 400 MHz, 298 K) of $^{3\text{-Ph}}$Ind$^{\#}$Li.

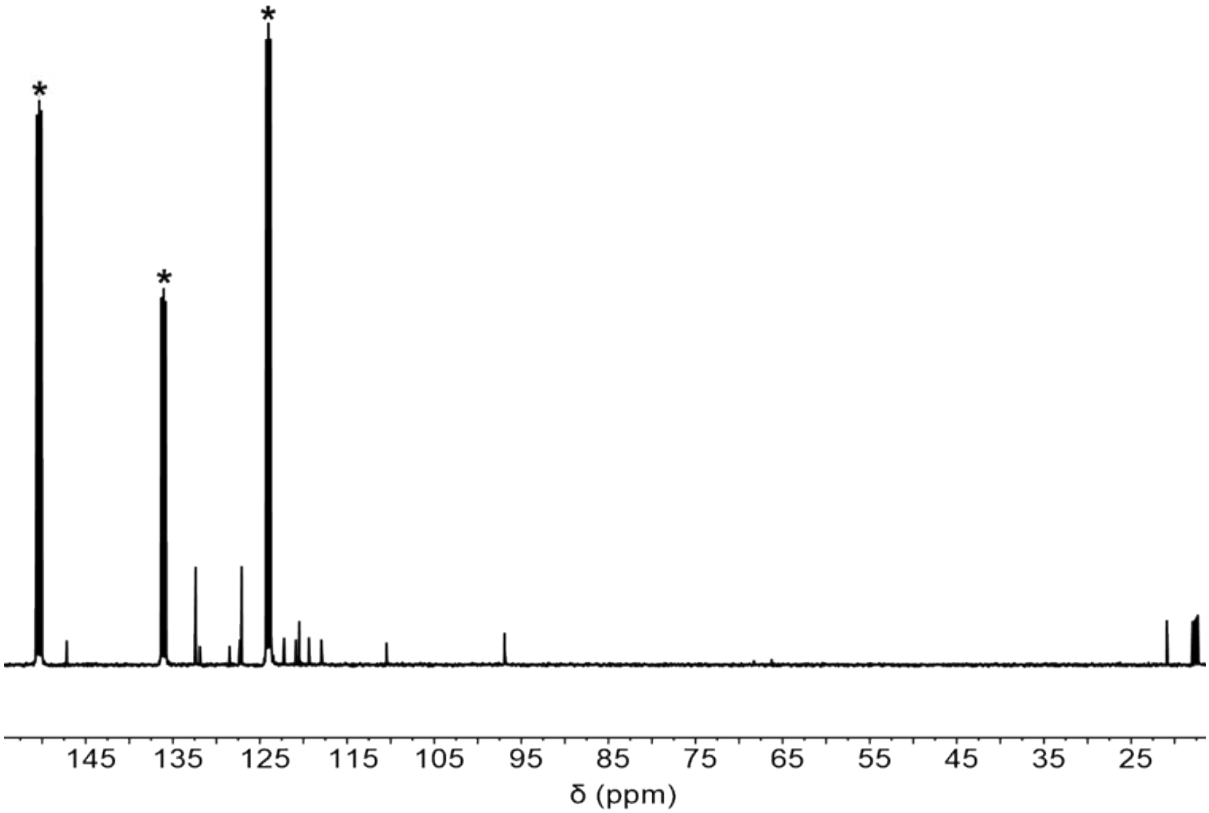

Fig. S10. ^{13}C{^{1}H} NMR spectrum (pyridine-d_5 (*), 101 MHz, 298 K) of $^{3\text{-Ph}}$Ind$^{\#}$Li.

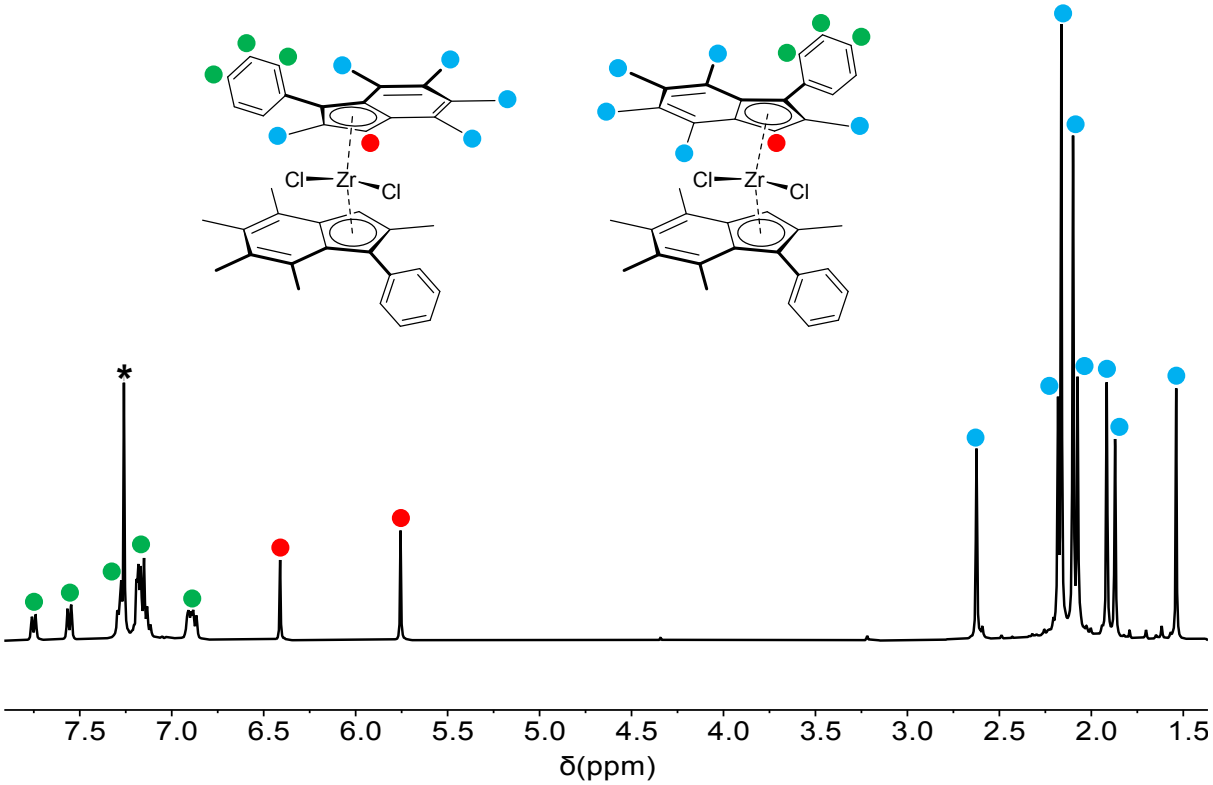

Fig. S11. ^{1}H NMR spectrum (chloroform-d_1 (*), 400 MHz, 298 K) of a 50:50 mixture of *rac*- and *meso*-($^{3\text{-Ph}}$Ind$^{\#}$)$_2$ZrCl$_2$ (**1**).

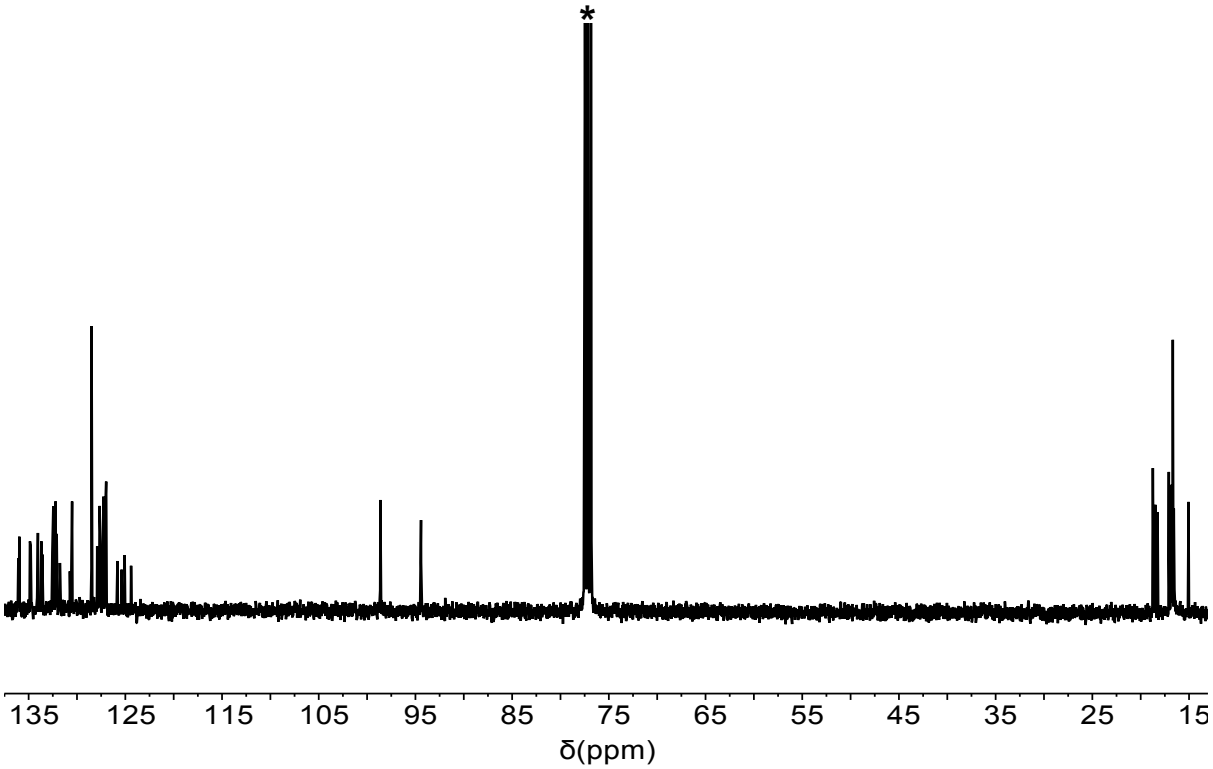

Fig. S12. ^{13}C{^{1}H} NMR spectrum (chloroform-d_1 (*), 101 MHz, 298 K) of a 50:50 mixture of *rac*- and *meso*-($^{3\text{-Ph}}$Ind$^{\#}$)$_2$ZrCl$_2$ (**1**).

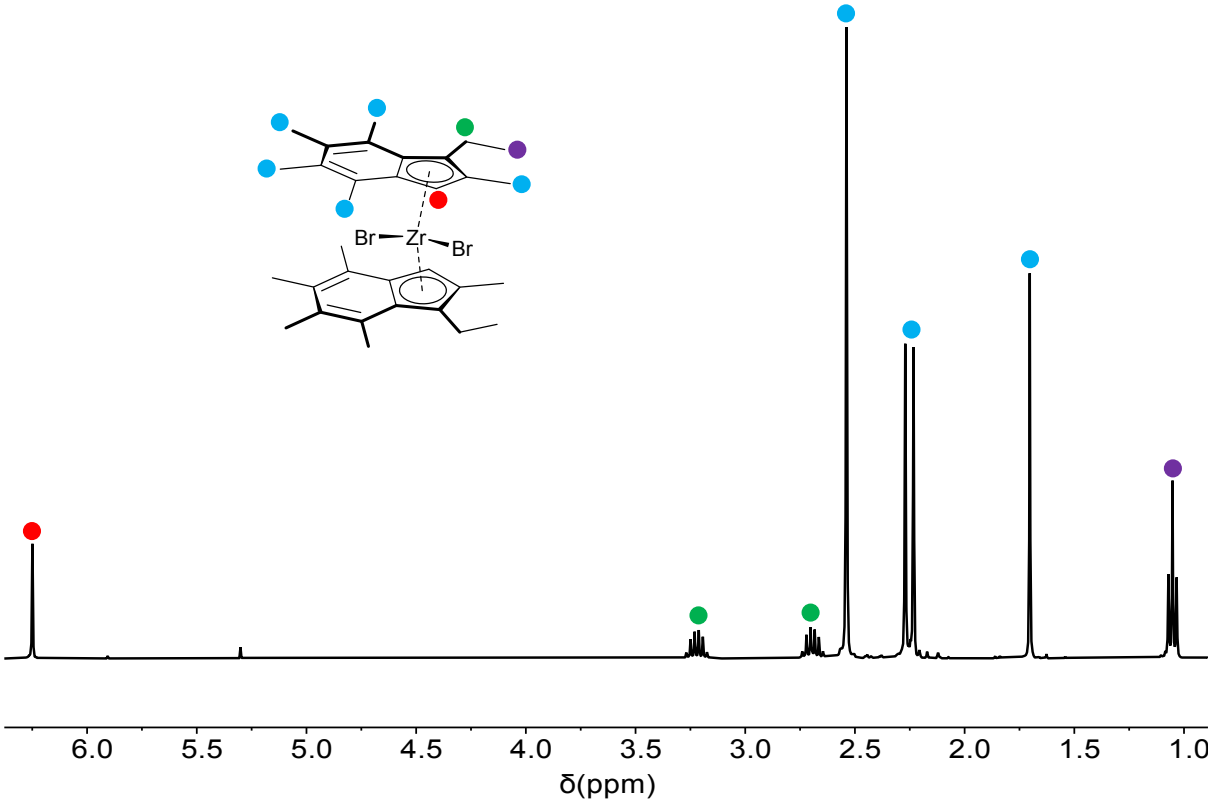

Fig. S13. ^{1}H NMR spectrum (chloroform-d_1, 400 MHz, 298 K) of *meso*-($^{3\text{-Et}}$Ind$^{\#}$)$_2$ZrBr$_2$ (***meso*-2**).

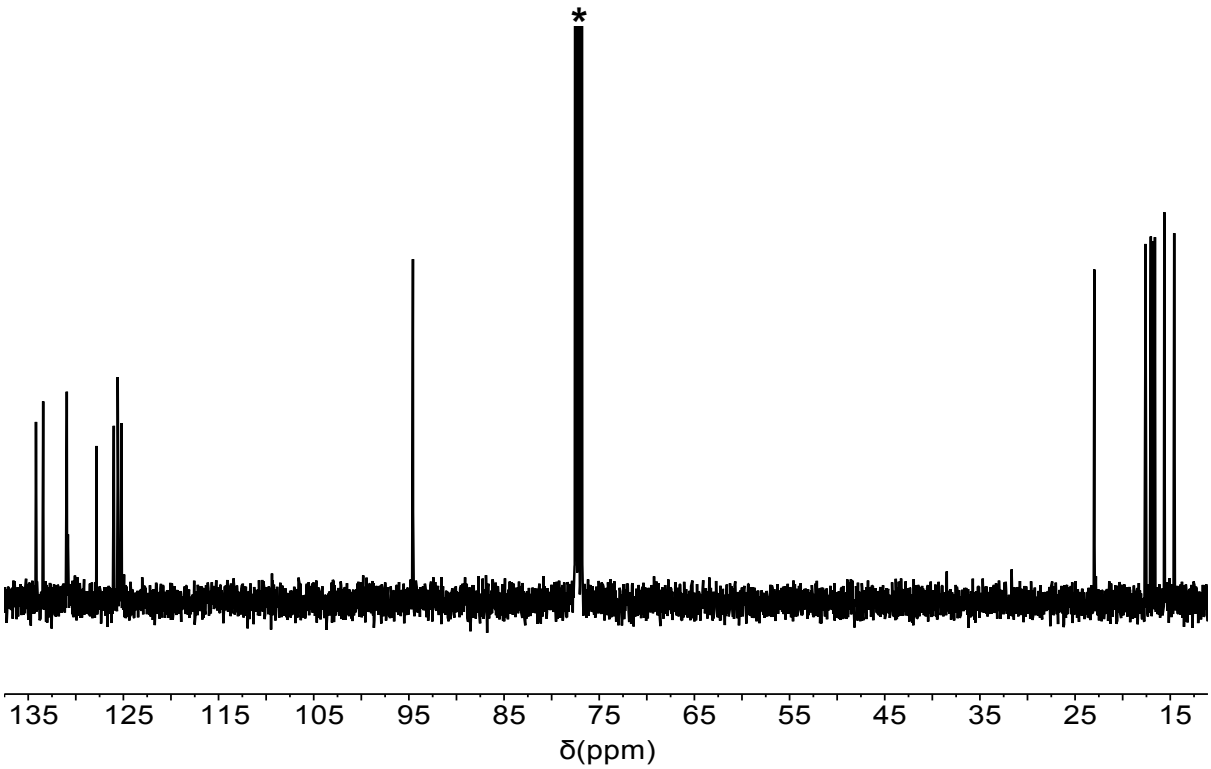

Fig. S14. ^{13}C{^{1}H} NMR spectrum (chloroform-d_1 (*), 101 MHz, 298 K) of *meso*-($^{3\text{-Et}}$Ind$^{\#}$)$_2$ZrBr$_2$ (***meso*-2**).

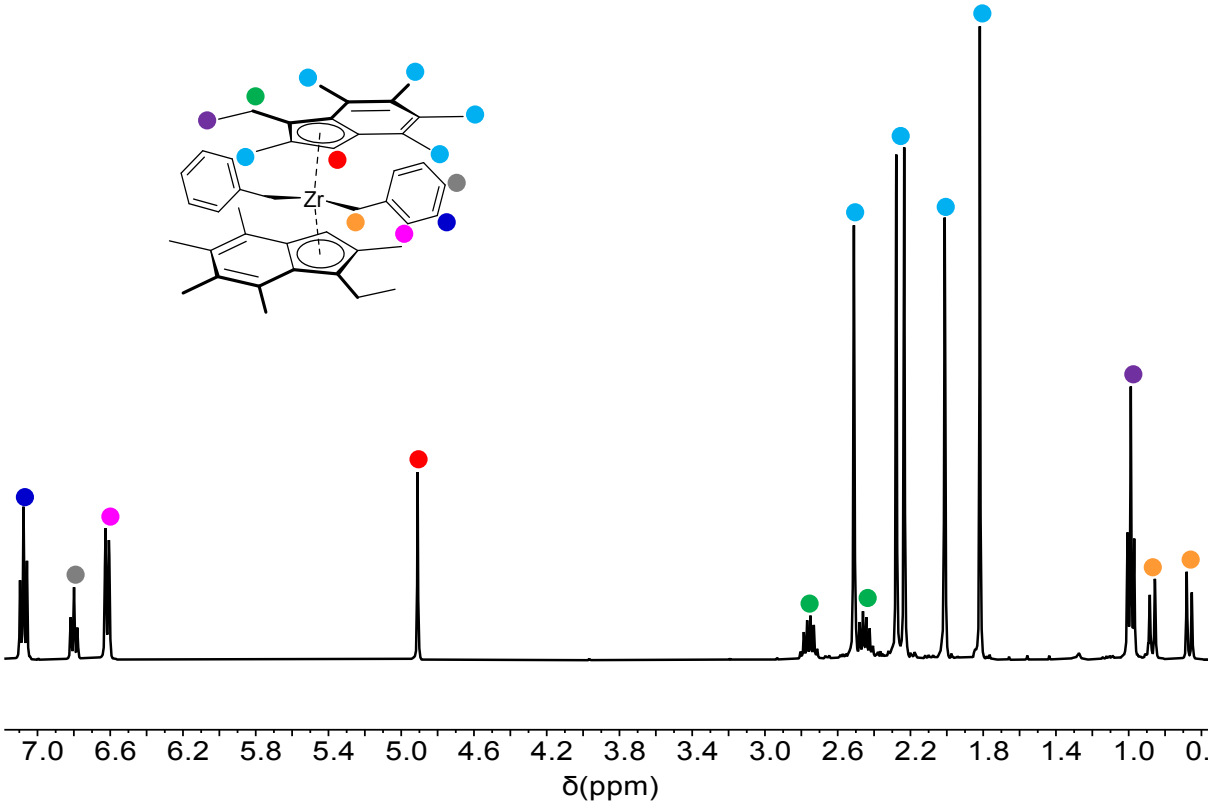

Fig. S15. ^{1}H NMR spectrum (chloroform-d_1 (*), 400 MHz, 298 K) of *rac*-($^{3\text{-Et}}$Ind$^{\#}$)$_2$Zr(CH$_2$Ph)$_2$ (***rac*-4**).

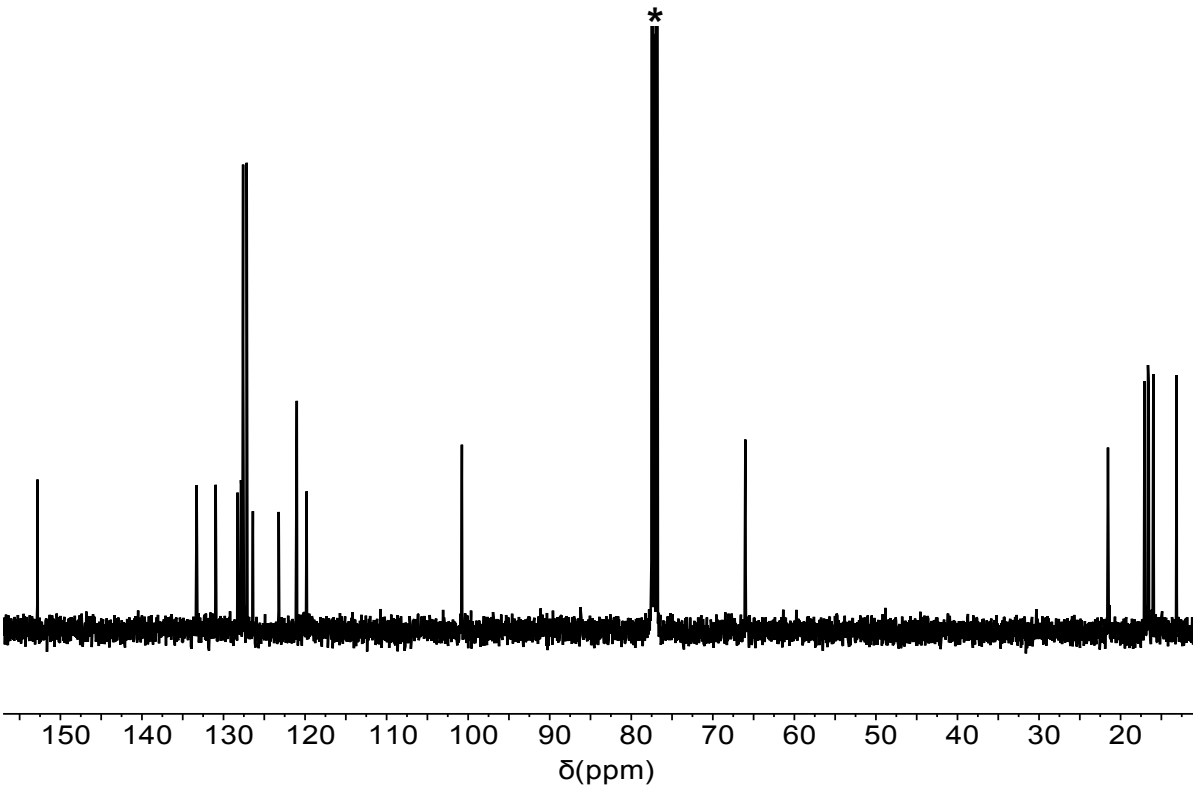

Fig. S16. ^{13}C{^{1}H} NMR spectrum (chloroform-d_1 (*), 101 MHz, 298 K) of *rac*-($^{3\text{-Et}}$Ind$^{\#}$)$_2$Zr(CH$_2$Ph)$_2$ (***rac*-4**).

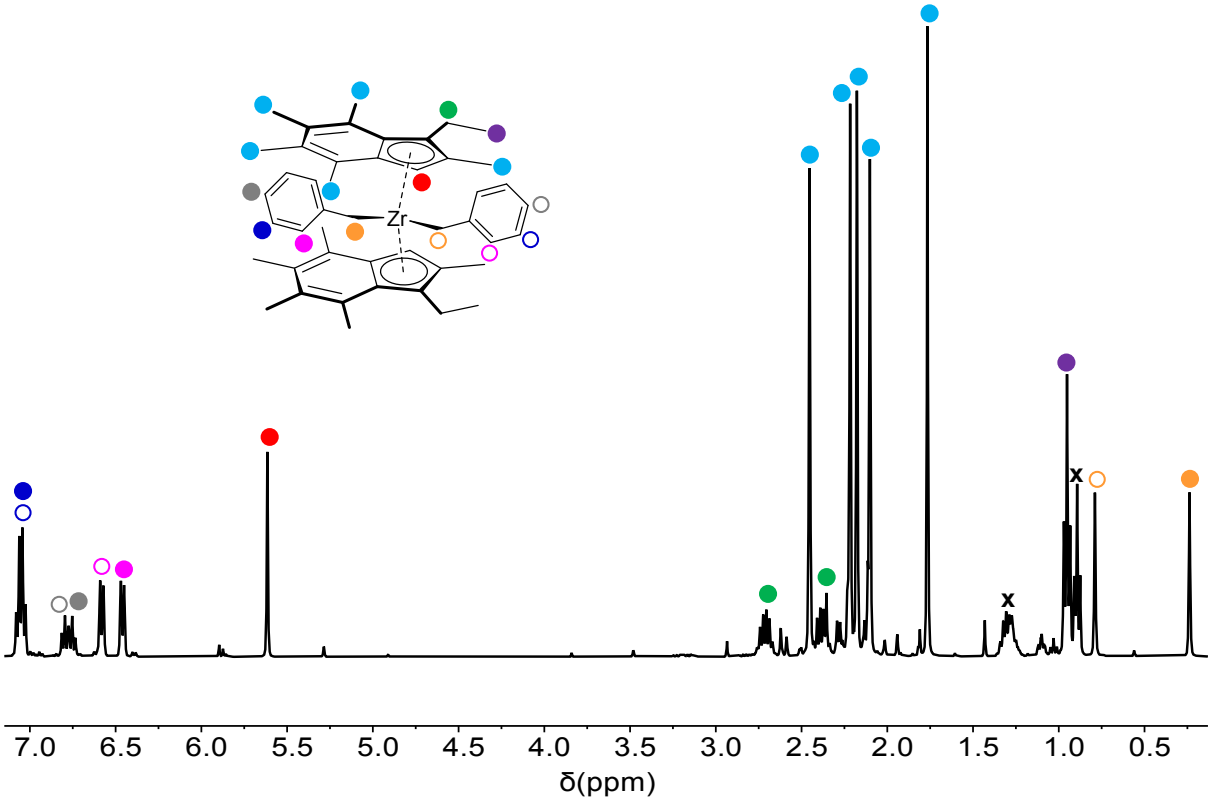

Fig. S17. ^{1}H NMR spectrum (chloroform-d_1, 400 MHz, 298 K) of *meso*-($^{3\text{-Et}}$Ind$^{\#}$)$_2$Zr(CH$_2$Ph)$_2$ (***meso*-4**). x detonates residual pentane.

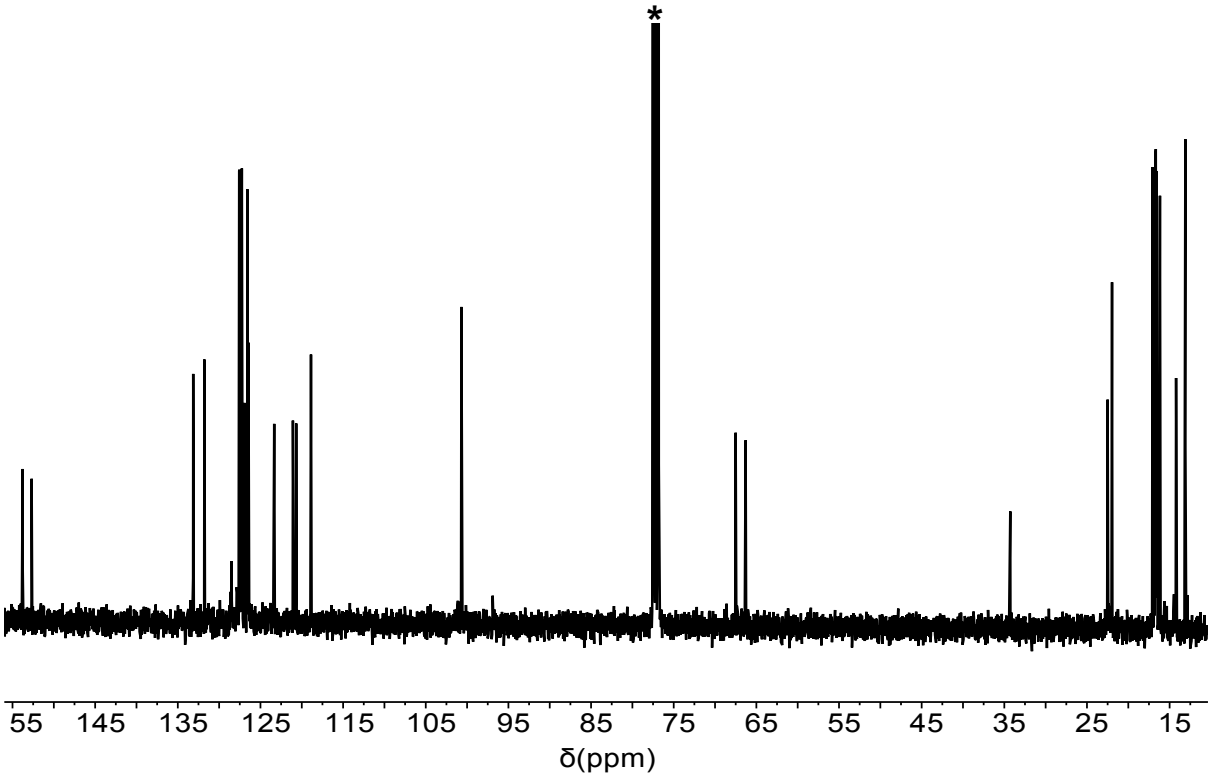

Fig. S18. ^{13}C{^{1}H} NMR spectrum (chloroform-d_1 (*), 101 MHz, 298 K) of *meso*-($^{3\text{-Et}}$Ind$^{\#}$)$_2$Zr(CH$_2$Ph)$_2$ (***meso*-4**). * detonates residual pentane.

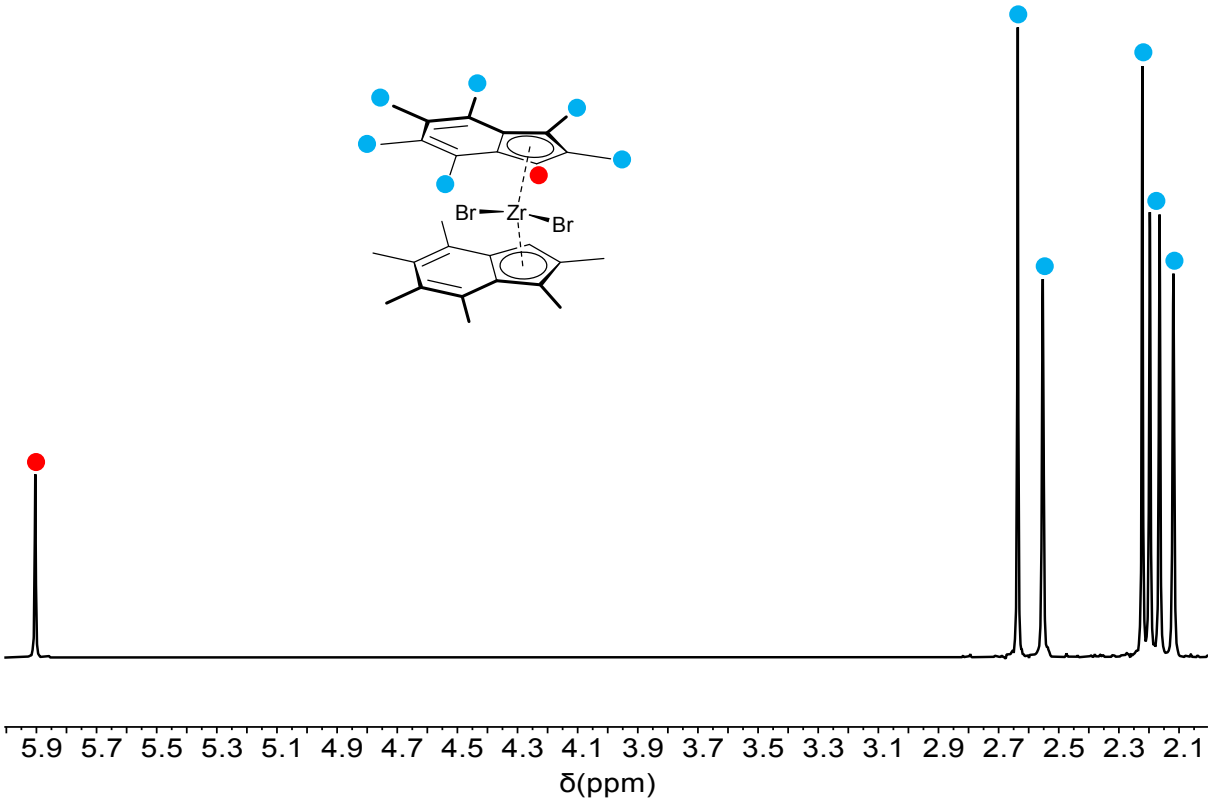

Fig. S19. ^{1}H NMR spectrum (chloroform-d_1, 400 MHz, 298 K) of *meso*-($^{3\text{-Me}}$Ind$^{\#}$)$_2$ZrBr$_2$ (***meso*-5**).

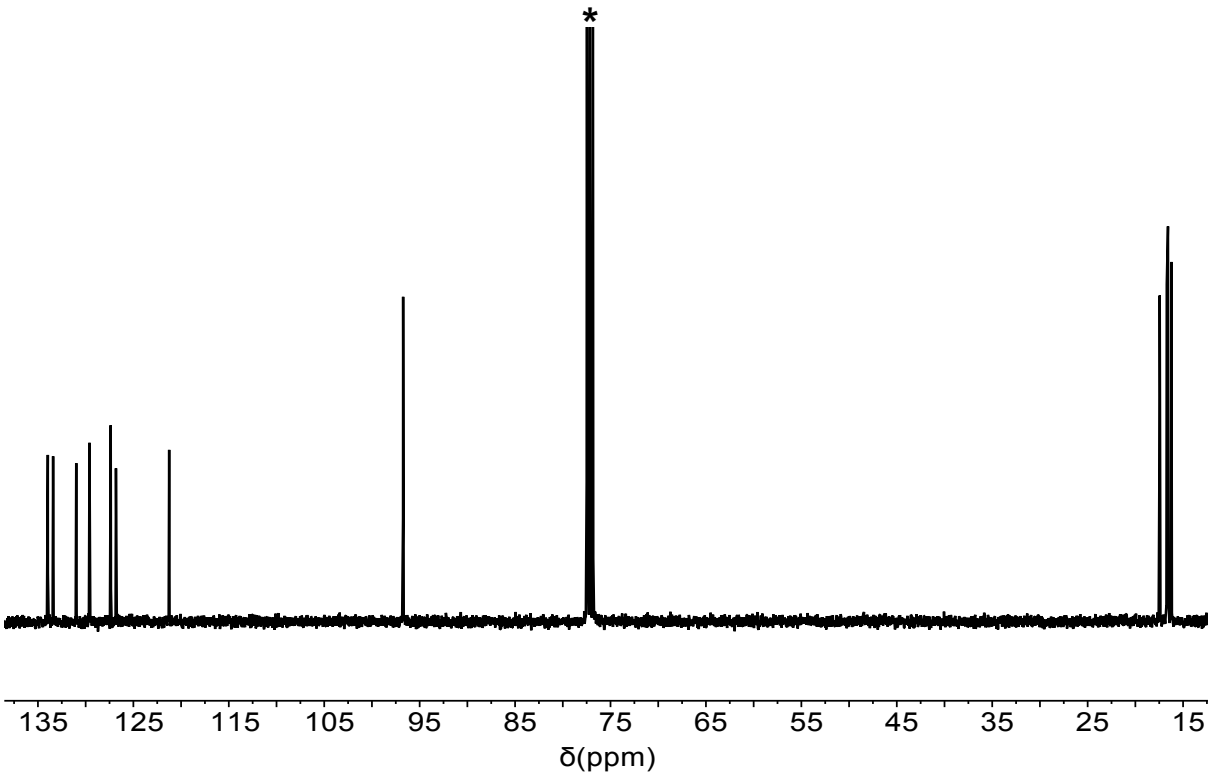

Fig. S20. ^{13}C{^{1}H} NMR spectrum (chloroform-d_1 (*), 101 MHz, 298 K) of *meso*-($^{3\text{-Me}}$Ind$^{\#}$)$_2$ZrBr$_2$ (***meso*-5**).

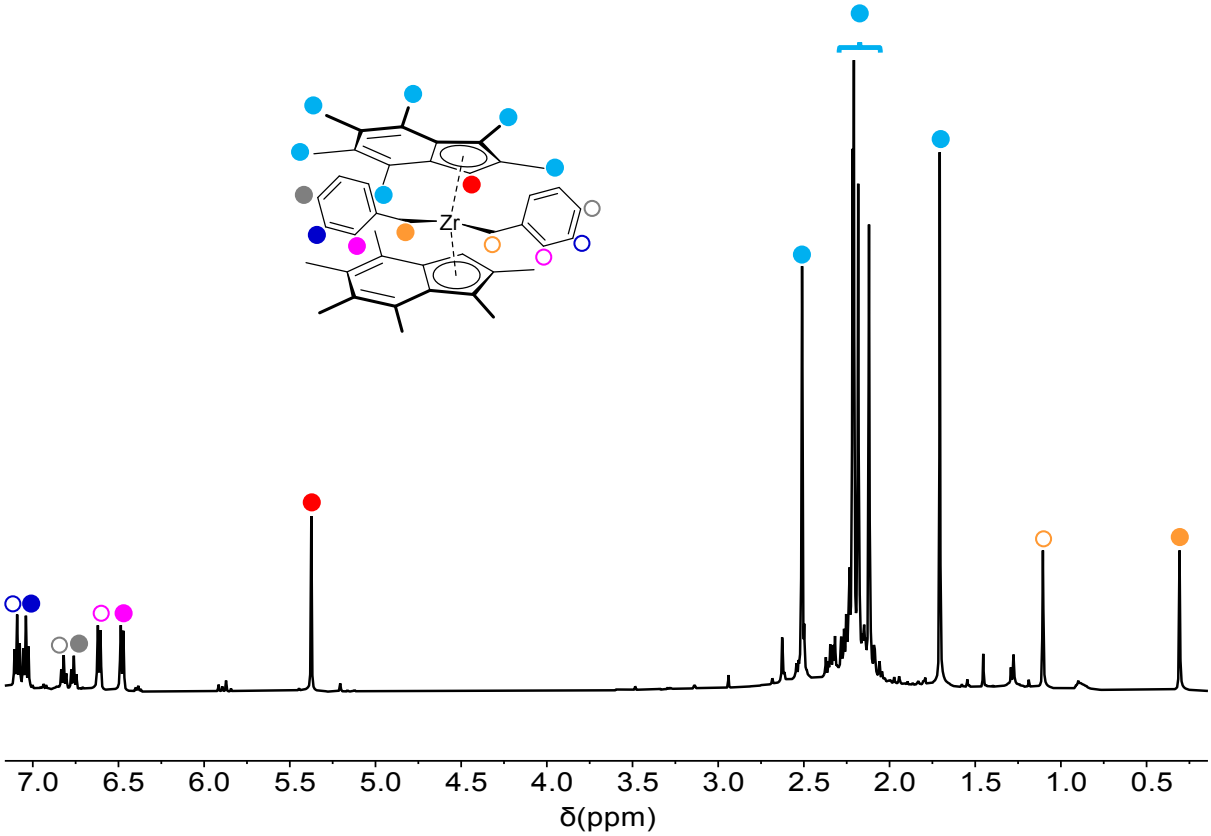

Fig. S21. ^{1}H NMR spectrum (chloroform-d_1, 500 MHz, 298 K) of *meso*-($^{3\text{-Me}}$Ind$^{\#}$)$_2$Zr(CH$_2$Ph)$_2$ (***meso*-6**).

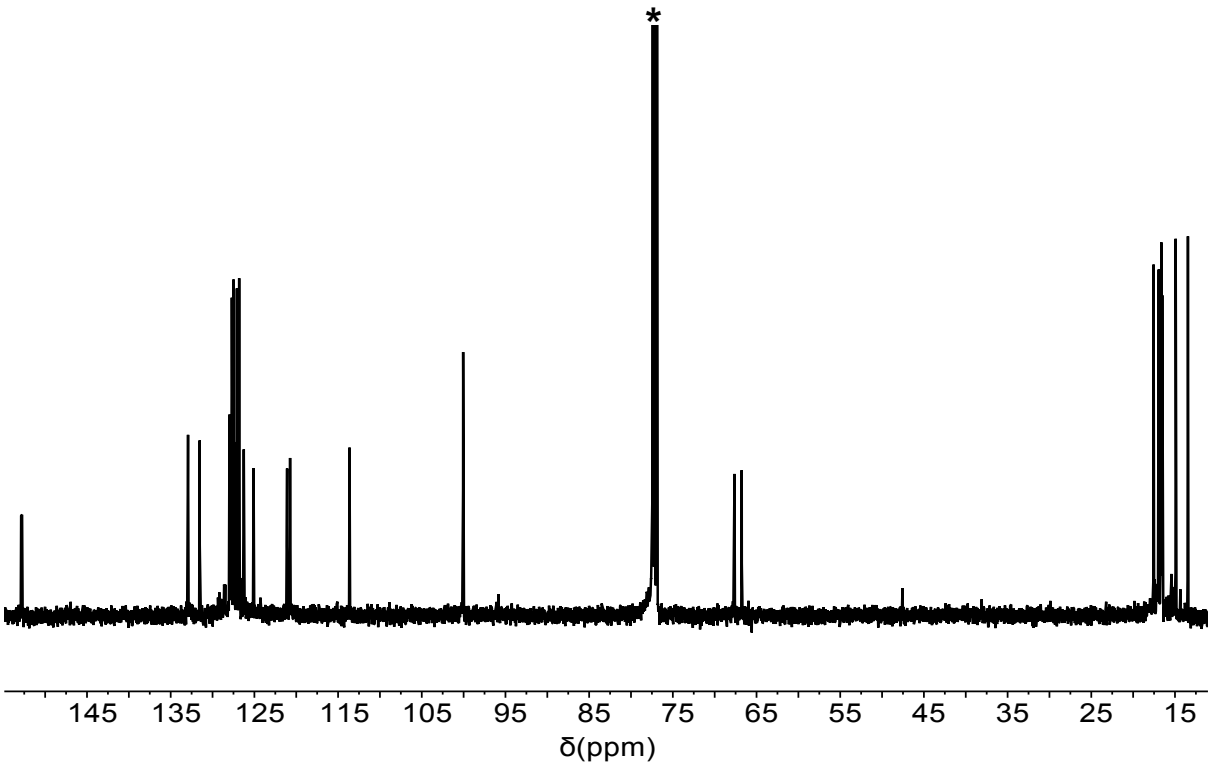

Fig. S22. ^{13}C{^{1}H} NMR spectrum (chloroform-d_1 (*), 125 MHz, 298 K) of *meso*-($^{3\text{-Me}}$Ind$^{\#}$)$_2$Zr(CH$_2$Ph)$_2$ (***meso*-6**).

4. Crystallographic data

4.1 Crystallographic details

Crystals were mounted on MiTeGen MicroMounts using a perfluoropolyether oil (Fomblin YR-1800, Alfa Aesar), rapidly transferred to a goniometer head on a diffractometer fitted with an Oxford Cryosystems Cryostream open-flow nitrogen cooling device and cooled 150 K.[3]

Two diffractometer setups were used:

1) An Enraf-Nonius Kappa CCD diffractometer using graphite monochromated Mo K_α radiation (λ = 0.71073 Å). Raw frame data were reduced using DENZO-SMN package,[4] and corrected for absorption using SORTAV.[5] Intensity data were collected using a multi-scan method with SCALEPACK (within DENZO-SMN).

2) An Oxford Diffraction Supernova diffractometer using multilayer, orthogonal, micro-focus Cu K_α radiation (λ = 1.5405 Å). Raw frame data were collected, reduced and processed using CrysAlisPRO.[6]

The structures were solved using direct methods (SHELXS)[7] or a charge flipping algorithm (SUPERFLIP)[8] and refined using a full-matrix least squares refinement on all F^2 data using CRYSTALS[9, 10] or Win-GX software suite.[11] In general, distances were calculated using the full variance/co-variance matrix. Dihedral angles were calculated using CCDC's Mercury[12] or PLATON.[13] Illustrations of the solid state molecular structures were created using ORTEP.[14]

4.2 Geometric parameters

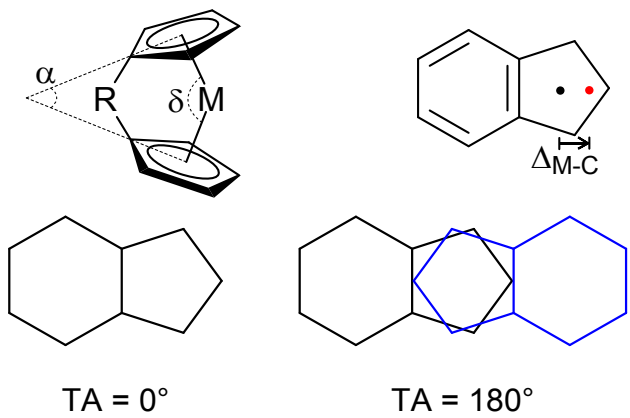

Figure S23. Visual representations of structural parameters.

4.3. Experimental crystallographic data

Table S1. Selected experimental crystallographic data for $^{3\text{-Ph}}$Ind$^{\#}$=O, $^{3\text{-Ph}}$Ind$^{\#}$H, *meso*-($^{3\text{-Et}}$Ind$^{\#}$)$_2$ZrBr$_2$ (***meso*-2**), *rac*-($^{3\text{-Et}}$Ind$^{\#}$)$_2$ZrCl$_2$ (***rac*-3**), *rac*-($^{3\text{-Et}}$Ind$^{\#}$)$_2$Zr(CH$_2$Ph)$_2$ (***rac*-4**), and *meso*-($^{3\text{-Et}}$Ind$^{\#}$)$_2$Zr(CH$_2$Ph)$_2$ (***meso*-4**).

	$^{3\text{-Ph}}$Ind$^{\#}$=O	**$^{3\text{-Ph}}$Ind$^{\#}$H**	***meso*-2**	***rac*-3**	***rac*-4**	***meso*-4**
			Crystal Data			
Chemical formula	$C_{20}H_{22}O$	$C_{20}H_{22}$	$C_{32}H_{42}Br_2Zr$	$C_{32}H_{42}Cl_2Zr$	$C_{46}H_{56}SiZr$	$C_{46}H_{56}Zr$
M_r	278.37	262.37	677.69	588.77	700.12	700.12
Crystal system	Orthorhombic	Monoclinic	Orthorhombic	Monoclinic	Monoclinic	Monoclinic
Space group	$Pna2_1$	$P2_1/c$	Pbca	$P2_1/c$	$P2_1/c$	P2/c
Temperature (K)	150	150	150	150	150	150
a (Å)	10.6474(13)	5.85320(10)	16.04490(10)	11.28590(10)	14.3118(2)	40.4192(6)
b (Å)	5.8091(7)	24.6468(5)	17.54360(10)	15.3811(2)	13.6443(2)	11.29010(10)
c (Å)	24.587(2)	10.7323 (2)	20.44350(10)	16.5363(2)	20.5174(4)	17.8001(3)
α (°)	90	90	90	90	90	90
β (°)	90	99.656(2)	90	94.5690(10)	109.185(2)	102.217(2)
γ (°)	90	90	90	90	90	90
V (Å^3)	1520.8	1526.33(5)	5754.55(6)	2861.41(6)	3784.01(11)	7938.9(2)
Z	4	4	8	4	4	8
Radiation type	Cu $K\alpha$	Cu $K\alpha$	Cu $K\alpha$	Cu $K\alpha$	Cu $K\alpha$	Cu $K\alpha$
μ (mm^{-1})	0.56	0.48	6.51	4.99	2.59	2.47
Crystal size (mm)	0.39 × 0.05 × 0.02	0.25 × 0.11 × 0.08	0.16 × 0.08 × 0.05	0.10 × 0.03 × 0.03	0.15 × 0. 13 × 0.11	0.24 × 0.21 × 0.10

Data Collection						
Diffractometer	SuperNova, Dual, Cu at zero, Atlas	SuperNova, Dual, Cu at zero, Atlas	SuperNova, Dual, Cu at zero, Atlas	SuperNova, Dual, Cu at zero, Atlas	SuperNova, Dual, Cu at zero, Atlas	SuperNova, Dual, Cu at zero, Atlas
Absorption correction	Multi-scan *CrysAlisPro* 1.171.38.41 (Rigaku Oxford Diffraction, 2015) Empirical absorption correction using spherical harmonics, implemented in SCALE3 ABSPACK scaling algorithm.	Multi-scan *CrysAlisPro* 1.171.38.41 (Rigaku Oxford Diffraction, 2015) Empirical absorption correction using spherical harmonics, implemented in SCALE3 ABSPACK scaling algorithm.	Multi-scan *CrysAlis*Pro 1.171.38.41 (Rigaku Oxford Diffraction, 2015) Empirical absorption correction using spherical harmonics, implemented in SCALE3 ABSPACK scaling algorithm.	Multi-scan *CrysAlis*Pro 1.171.38.41 (Rigaku Oxford Diffraction, 2015) Empirical absorption correction using spherical harmonics, implemented in SCALE3 ABSPACK scaling algorithm.	Multi-scan *CrysAlis*Pro 1.171.38.41 (Rigaku Oxford Diffraction, 2015) Empirical absorption correction using spherical harmonics, implemented in SCALE3 ABSPACK scaling algorithm.	Gaussian *CrysAlis*Pro 1.171.38.41 (Rigaku Oxford Diffraction, 2015) Empirical absorption correction using spherical harmonics, implemented in SCALE3 ABSPACK scaling algorithm.
T_{min}, T_{max}	0.512, 1.000	0.857, 1.000	0.673, 1.000	0.850, 1.000	0.884, 1.000	0.462, 1.000
No. of measured, independent and observed [$I > 2\sigma(I)$] reflections	6223, 2960, 2292	18491, 3125, 2691	68408, 5883, 5511	16185, 5841, 4958	75671, 7883 7100	80076, 16214, 15795
R_{int}	0.054	0.022	0.029	0.029	0.041	0.038
Refinement						
$R[F^2 > 2\sigma(F^2)]$, $wR(F^2)$, S	0.056, 0.166, 0.978	0.049, 0.153, 1.069	0.077, 0.079, 1.041	0.025, 0.060, 1.012	0.028, 0.075, 1.049	0.105, 0.254, 1.206
No. of reflections	2960	3125	5883	5841	7883	16214
No. of parameters	195	186	328	328	436	871
No. of restraints	1	0	0	0	0	0

$(\Delta/\sigma)_{max}$	0.000	0.000	0.001	0.002	0.000	0.000
$\Delta\rho_{max}$, $\Delta\rho_{min}$ (e Å^{-3})	0.21, −0.24	0.25, −0.18	1.86, −0.62	0.27, −0.54	0.42, −0.75	5.94, −1.98

Computer programs: CrysAlisPro 1.171.39.46 (Rigaku OD, 2018), CrysAlisPro 1.171.38.41 (Rigaku OD, 2015), SUPERFLIP Palatinus, L.; Chapuis, G. J. Appl. Cryst. 2007, 40, 786-790., *SIR92* Altomare, A.; Cascarano, G.; Giacovazzo, C.; Guagliardi, A. J. Appl. Cryst. 1994, 27, 435., SUPERFLIP. Palatinus, L.; Chapuis, G. J. Appl. Cryst. 2007, 40, 786-790., *SHELXL2014* (Sheldrick, 2014), *ORTEP-3 for Windows*. Farrugia, L. J. J. Appl. Cryst. 1997, 30, 565.

Table S2. Selected experimental crystallographic data for, *meso*-($^{3\text{-Me}}$Ind$^{\#}$)$_2$ZrBr$_2$ (***meso*-5**), *meso*-($^{3\text{-Me}}$Ind$^{\#}$)$_2$Zr(CH$_2$Ph)$_2$ (***meso*-6**).

	***meso*-5**	***meso*-6**
Chemical formula	$C_{30}H_{38}Br_2Zr$	$C_{47.50}H_{56}Zr$
M_r	649.64	718.14
Crystal system	Monoclinic	Monoclinic
Space group	$P2_1/n$	$C2/c$
Temperature (K)	150	150
a (Å)	12.49280(10)	23.5240(7)
b (Å)	14.83150(10)	12.9247(3)
c (Å)	14.58980(10)	25.9982(8)
α (°)	90	90
β (°)	98.3100	112.710(4)
γ (°)	90	90
V (Å^3)	2674.90(3)	7291.7(4)
Z	4	8
Radiation type	Mo $K\alpha$	Cu $K\alpha$
μ (mm^{-1})	3.42	2.70
Crystal size (mm)	0.22 × 0.20 × 0.15	0.09 × 0.07 × 0.04
Diffractometer	KappaCCD	SuperNova, Dual, Cu at zero, Atlas
Absorption correction	Multi-scan from symmetry-related measurements using	Multi-scan *CrysAlis*Pro 1.171.38.41 (Rigaku Oxford Diffraction,

	Sortav (Blessing 1995)	2015) Empirical absorption correction using spherical harmonics, implemented in SCALE3 ABSPACK scaling algorithm.
T_{min}, T_{max}	0.906, 1.000	0.873, 1.000
No. of measured, independent and observed [$I > 2\sigma(I)$] reflections	11942, 6098, 5374	16598, 7392, 6405
R_{int}	0.026	0.023
$R[F^2 > 2\sigma(F^2)]$, $wR(F^2)$, S	0.029, 0.072, 1.054	0.025, 0.063, 1.034
No. of reflections	6098	7392
No. of parameters	309	452
No. of restraints	0	0
$(\Delta/\sigma)_{max}$	0.002	0.001
$\Delta\rho_{max}$, $\Delta\rho_{min}$ (e Å^{-3})	0.48, −0.79	0.33, −0.44

Computer programs: CrysAlisPro 1.171.39.46 (Rigaku OD, 2018), CrysAlisPro 1.171.38.41 (Rigaku OD, 2015), SUPERFLIP Palatinus, L.; Chapuis, G. J. Appl. Cryst. 2007, 40, 786-790., *SIR92* Altomare, A.; Cascarano, G.; Giacovazzo, C.; Guagliardi, A. J. Appl. Cryst. 1994, 27, 435., SUPERFLIP. Palatinus, L.; Chapuis, G. J. Appl. Cryst. 2007, 40, 786-790., *SHELXL2014* (Sheldrick, 2014), *ORTEP-3 for Windows*. Farrugia, L. J. J. Appl. Cryst. 1997, 30, 565.

5. Polymerisation data

Table S3. Slurry-phase ethylene polymerisation using sMAO-($^{3\text{-Ph}}$Ind$^{\#}$)$_2$ZrCl$_2$ (**1$_{sMAO}$**).

Temperature (°C)	Activity (kg_{PE} mol_{Zr}^{-1} h^{-1} bar^{-1})	M_w (kg mol^{-1})	M_w/M_n
50	54 ± 18	-	-
60	46 ± 1	-	-
70	41 ± 2	-	-
80	36 ± 1	-	-
90	35 ± 0	-	-

Polymerisation conditions: ethylene (2 bar), pre-catalyst (10 mg), hexane (50 mL), $[Al_{sMAO}]_0/[Zr]_0$ = 200, TiBA (1000 eq.), and 30 minutes.

Table S4. Slurry-phase ethylene polymerisation using sMAO-*meso*-($^{3\text{-Et}}$Ind$^{\#}$)$_2$ZrBr$_2$ (***meso*-2$_{sMAO}$**).

Temperature (°C)	Activity (kg_{PE} mol_{Zr}^{-1} h^{-1} bar^{-1})	M_w (kg mol^{-1})	M_w/M_n
50	557 ± 16	503	8.1
60	525 ± 24	350	7.9
70	452 ± 28	284	7.2
80	320 ± 9	209	6.9
90	225 ± 40	212	7.7

Polymerisation conditions: ethylene (2 bar), pre-catalyst (10 mg), hexane (50 mL), $[Al_{sMAO}]_0/[Zr]_0$ = 200, TiBA (1000 eq.), and 30 minutes.

Table S5. Slurry-phase ethylene polymerisation using sMAO-*rac*-($^{3\text{-Et}}$Ind$^{\#}$)$_2$ZrCl$_2$ (***rac*-3$_{\mathbf{sMAO}}$**).

Temperature (°C)	**Activity (kg_{PE} mol_{Zr}^{-1} h^{-1} bar^{-1})**	**M_w (kg mol^{-1})**	**M_w/M_n**
50	1072 ± 10	391	5.0
60	858 ± 5	298	5.4
70	561 ± 25	190	5.3
80	382 ± 7	-	-
90	239 ± 14	-	-

Polymerisation conditions: ethylene (2 bar), pre-catalyst (10 mg), hexane (50 mL), $[Al_{sMAO}]_0/[Zr]_0$ = 200, TiBA (1000 eq.), and 30 minutes.

Table S6. Slurry-phase ethylene polymerisation using sMAO-*meso*-($^{3\text{-Et}}$Ind$^{\#}$)$_2$ZrCl$_2$ (***meso*-3$_{\mathbf{sMAO}}$**).

Temperature (°C)	**Activity (kg_{PE} mol_{Zr}^{-1} h^{-1} bar^{-1})**	**M_w (kg mol^{-1})**	**M_w/M_n**
50	690 ± 5	406	7.3
60	651 ± 20	320	6.9
70	526 ± 0	232	7.2
80	385 ± 9	206	8.2
90	249 ± 3	164	8.0

Polymerisation conditions: ethylene (2 bar), pre-catalyst (10 mg), hexane (50 mL), $[Al_{sMAO}]_0/[Zr]_0$ = 200, TiBA (1000 eq.), and 30 minutes.

Table S7. Slurry-phase ethylene polymerisation using sMAO-*rac*-($^{3\text{-Et}}$Ind$^{\#}$)$_2$Zr(CH$_2$Ph)$_2$ (***rac*-4$_{\mathbf{sMAO}}$**).

Temperature (°C)	**Activity (kg$_{\mathbf{PE}}$ mol$_{\mathbf{Zr}}^{-1}$ h^{-1} bar^{-1})**	***M*$_{\mathbf{w}}$ (kg mol^{-1})**	***M*$_{\mathbf{w}}$/*M*$_{\mathbf{n}}$**
50	1119 ± 0	381	5.7
60	846 ± 0	275	5.4
70	486 ± 24	217	6.8
80	272 ± 23	142	6.0
90	123 ± 10	113	7.0

Polymerisation conditions: ethylene (2 bar), pre-catalyst (10 mg), hexane (50 mL), $[Al_{sMAO}]_0/[Zr]_0$ = 200, TiBA (1000 eq.), and 30 minutes.

Table S8. Slurry-phase ethylene polymerisation using sMAO-*meso*-($^{3\text{-Et}}$Ind$^{\#}$)$_2$Zr(CH$_2$Ph)$_2$ (***meso*-4$_{\mathbf{sMAO}}$**).

Temperature (°C)	**Activity (kg$_{\mathbf{PE}}$ mol$_{\mathbf{Zr}}^{-1}$ h^{-1} bar^{-1})**	***M*$_{\mathbf{w}}$ (kg mol^{-1})**	***M*$_{\mathbf{w}}$/*M*$_{\mathbf{n}}$**
50	877 ± 34	345	5.0
60	834 ± 44	266	5.0
70	657 ± 24	202	5.0
80	404 ± 39	129	4.7
90	270 ± 17	124	5.5

Polymerisation conditions: ethylene (2 bar), pre-catalyst (10 mg), hexane (50 mL), $[Al_{sMAO}]_0/[Zr]_0$ = 200, TiBA (1000 eq.), and 30 minutes.

Table S9. Slurry-phase ethylene polymerisation using sMAO-*meso*-($^{3\text{-Me}}$Ind$^{\#}$)$_2$ZrBr$_2$ (***meso*-5$_{\mathbf{sMAO}}$**).

Temperature (°C)	**Activity (kg_{PE} mol_{Zr}^{-1} h^{-1} bar^{-1})**	**M_w (kg mol^{-1})**	**M_w/M_n**
50	705 ± 8	395	5.6
60	874 ± 36	328	5.6
70	927 ± 34	199	4.2
80	612 ± 29	218	6.4
90	340 ± 4	133	6.0

Polymerisation conditions: ethylene (2 bar), pre-catalyst (10 mg), hexane (50 mL), $[Al_{sMAO}]_0/[Zr]_0$ = 200, TiBA (1000 eq.), and 30 minutes.

6. References

1. Bailey, P. J.; Coxall, R. A.; Dick, C. M.; Fabre, S.; Henderson, L. C.; Herber, C.; Liddle, S. T.; Loroño-González, D.; Parkin, A.; Parsons, S., The first structural characterisation of a group 2 metal alkylperoxide complex: comments on the cleavage of dioxygen by magnesium alkyl complexes. *Chem. Eur. J.* **2003,** *9* (19), 4820-4828.
2. Arnold, T. A. Q.; Buffet, J.-C.; Turner, Z. R.; O'Hare, D., Synthesis, characterisation, and polymerisation studies of hexamethylindenyl zirconocenes and hafnocenes. *J. Organomet. Chem.* **2015,** *792*, 55-65.
3. Cosier, J.; Glazer, A. M., A nitrogen-gas-stream cryostat for general X-ray diffraction studies. *J. Appl. Crystallogr.* **1986,** *19*, 105-107.
4. Otwinowski, Z.; Minor, W., Processing of X-ray diffraction data collected in oscillation mode. *Methods Enzymol.* **1997,** *276*, 307-326.
5. Blessing, R., An empirical correction for absorption anisotropy. *Acta Crystallogr., Sect. A: Found. Adv.* **1995,** *51* (1), 33-38.
6. CrysAlisPRO, Oxford Diffraction /Agilent Technologies UK Ltd: Yarnton, England.
7. Sheldrick, G., A short history of SHELX. *Acta Crystallogr., Sect. A: Found. Adv.* **2008,** *64* (1), 112-122.
8. Palatinus, L.; Chapuis, G., SUPERFLIP - a computer program for the solution of crystal structures by charge flipping in arbitrary dimensions. *J. Appl. Crystallogr.* **2007,** *40*, 786-790.
9. Betteridge, P. W.; Carruthers, J. R.; Cooper, R. I.; Prout, K.; Watkin, D. J., CRYSTALS version 12: Software for guided crystal structure analysis. *J. Appl. Crystallogr.* **2003,** *36* (6), 1487.
10. Cooper, R. I.; Thompson, A. L.; Watkin, D. J., CRYSTALS enhancements: Dealing with hydrogen atoms in refinement. *J. Appl. Crystallogr.* **2010,** *43* (5 Part 1), 1100-1107.
11. Farrugia, L. J., WinGX suite for small-molecule single-crystal crystallography. *J. Appl. Crystallogr.* **1999,** *32* (4), 837-838.
12. Macrae, C. F.; Bruno, I. J.; Chisholm, J. A.; Edgington, P. R.; McCabe, P.; Pidcock, E.; Rodriguez-Monge, L.; Taylor, R.; van de Streek, J.; Wood, P. A., Mercury CSD 2.0 - new features for the visualization and investigation of crystal structures. *J. Appl. Crystallogr.* **2008,** *41* (2), 466-470.
13. Spek, A. L., Single-crystal structure validation with the program PLATON. *J. Appl. Crystallogr.* **2003,** *36*, 7-13.
14. Farrugia, L. J., WinGX and ORTEP for Windows: an update. *J. Appl. Crystallogr.* **2012,** *45*, 849-854.